Aging and Disease
www.aginganddisease.org
Early access date: November 9, 2026
http://dx.doi.org/10.14336/AD.2026.1294

Review

The Microglial Lipid–Immune Axis in Brain Aging: Adaptive Lipid Handling and Metabolic Dysfunction in Lipid-Droplet-Accumulating Microglia

Xintong Wang[1,2,3], Anran Lv[3], Yu Tian[3], Dongna Li[1,2,3], Xueji Fan[3], Yuqian Wang[3], Pengwei Zhuang[1,2,3*], Yanjun Zhang[1,2,3*]

[1]First Teaching Hospital of Tianjin University of Traditional Chinese Medicine, Tianjin, China. [2]National Clinical Research Center for Chinese Medicine, Tianjin, China. [3]State Key Laboratory of Chinese Medicine Modernization, Tianjin University of Traditional Chinese Medicine, Tianjin, China.

[Received August 8, 2026; Revised November 1, 2026; Accepted November 5, 2026]

ABSTRACT: Microglia in the aging brain process lipids released during membrane and myelin turnover. Lipid droplets can buffer this demand, but lipid retention also accompanies defective phagocytosis and inflammatory responses. This review critically compares the substrates, perturbations, and functional endpoints underlying these observations. We examine cholesterol esterification and export, fatty-acid activation and triacylglycerol synthesis, and lipid mobilization through lipolysis and lipophagy in relation to TREM2–TYROBP/DAP12–SYK signaling, APOE genotype, and local substrate supply. Physiological-aging studies are distinguished from demyelination, Alzheimer's disease, and Parkinson's disease models. Quantitative comparisons show why inhibiting storage can improve selected amyloid-associated phenotypes while impaired storage can compromise myelin repair. We use the established distinction between lipid pools and metabolic flux to assess what each experiment demonstrates: altered droplet abundance, a specific processing defect, or recovery of a cellular task. We propose a reporting framework covering droplet burden, transcriptional state, metabolic function, and cellular performance, with missing measurements retained explicitly and no claim of validated diagnostic thresholds. Intervention evidence is assessed by the reaction perturbed, dose and duration, target validation, delivery route, and measured benefit. The resulting synthesis identifies supported mechanisms and unresolved causal steps, providing a practical basis for selecting and evaluating interventions without treating droplet reduction as a universal therapeutic endpoint.

Keywords: Brain aging, Microglia, Lipid flux, LDAM, TREM2–SYK, APOE genotype, Pharmacology

1. Introduction

Population aging has made age-associated neurological decline a major research concern [1, 2]. Brain aging changes energy metabolism, synaptic plasticity, and damage clearance and increases susceptibility to Alzheimer's disease (AD) and Parkinson's disease (PD) [3, 4]. Oxidative stress, mitochondrial injury, loss of proteostasis, and chronic inflammation interact across these processes [1]. Lipid metabolism connects them: brain cells must maintain membranes and myelin while disposing of lipids released during turnover and injury.

Microglia maintain tissue homeostasis through surveillance, synaptic remodeling, and phagocytosis [5]. Their heterogeneous responses to aging and disease include both adaptation to injury and loss of function under sustained stress [6]. For lipid-rich cargo, the consequence of uptake depends on subsequent degradation, reuse, and export. A cell can therefore increase phagocytic entry while retaining more poorly processed material. This distinction between uptake and completed clearance is central to interpreting microglial activation.

Cholesterol, sphingolipids, phospholipids, and polyunsaturated fatty acids (PUFAs) support brain

***Correspondence should be addressed to:** Dr. Pengwei Zhuang (Email: zhuangpengwei@163.com) and Dr. Yanjun Zhang (zyjsunye@163.com), First Teaching Hospital of Tianjin University of Traditional Chinese Medicine, Tianjin, China.

Copyright: © 2026 Wang X., et al. This is an open-access article distributed under the terms of the Creative Commons Attribution License, which permits unrestricted use, distribution, and reproduction in any medium, provided the original author and source are credited.

membranes, myelin, and signaling [7, 8]. Changes in transport, storage, and peroxidation during aging vary by region and cell type [9, 10]. Similar droplet counts can arise from temporary storage with rapid turnover or from substrate retention with poor disposal. Lipid identity and the rates of uptake, esterification, mobilization, oxidation, and export are therefore central to interpreting these observations [11, 12].

TREM2, APOE, CD36, and LXR–ABCA1/ABCG1 networks link lipid recognition to survival, phagocytosis, and export [7, 13, 14]. During sustained phagocytic challenge, receptor-mediated uptake must be matched by downstream processing to achieve tissue clearance [10, 14]. The worsening of cholesterol-handling defects after TREM2 loss also places this receptor within the adaptive response to metabolic demand.

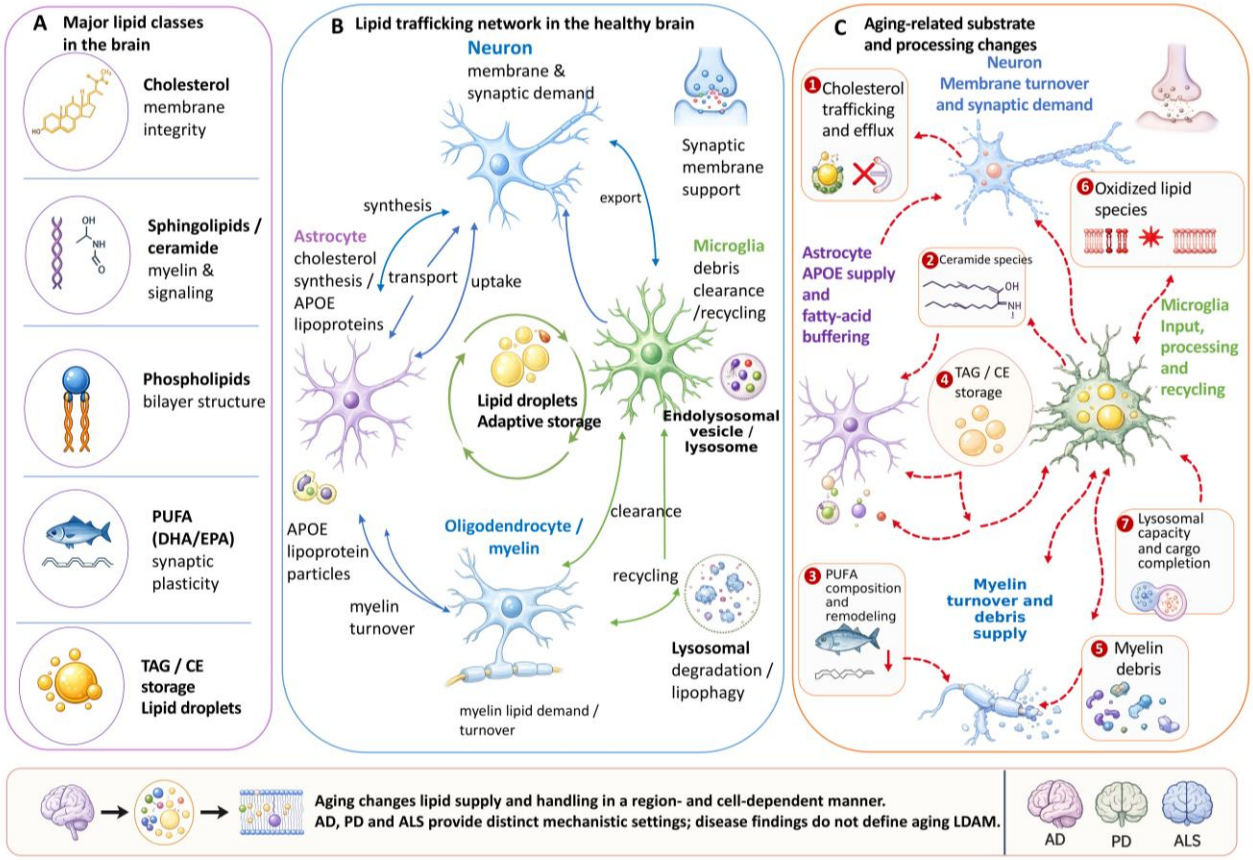


Figure 1. Brain lipid sources, trafficking and aging contexts. (A) Major brain lipid classes and their principal roles in membranes, myelin, signaling, and neutral-lipid storage. **(B)** Intercellular lipid handling: astrocytic APOE-containing lipoproteins and fatty-acid buffering, neuronal membrane maintenance, oligodendrocyte myelin turnover, and microglial processing of cellular and myelin-derived cargo. **(C)** Aging-related changes in substrate supply and organelle function. Cell colors retain the identities shown in the figure. Solid arrows identify transfer or processing routes; dashed links identify context-dependent alterations. Abbreviations: AD, Alzheimer's disease; ALS, amyotrophic lateral sclerosis; APOE, apolipoprotein E; CE, cholesteryl ester; DHA, docosahexaenoic acid; EPA, eicosapentaenoic acid; LDAM, lipid-droplet-accumulating microglia; PD, Parkinson's disease; PUFA, polyunsaturated fatty acid; TAG, triacylglycerol.

Here, the microglial lipid–immune axis refers to reciprocal regulation between lipid processing and immune function. Links among cholesterol trafficking, lipid recognition, and inflammatory signaling have been studied in several models [11, 13, 14]. The identification of lipid-droplet-accumulating microglia (LDAM) in aged mice associated droplet accumulation with impaired phagocytic uptake, elevated reactive oxygen species (ROS), and inflammatory output [15, 16]. The interpretation of these observations depends on the substrate and task examined, as illustrated by the quantitative comparisons in Sections 4 and 6.

Recent reviews have synthesized microglial lipid metabolism, neuroinflammation, droplet biology, and therapeutic targets [10, 11, 16-18]. They also discuss lipid turnover, the balance between supply and utilization, and the organelle capacity needed for functional restoration [16, 19, 20]. Building on this work, the present review

compares primary experiments by lipid substrate, reaction perturbed, quantitative result, and functional endpoint, with physiological-aging evidence considered separately from disease-model mechanisms. This comparison addresses how apparently similar droplet changes support different conclusions about processing and intervention.

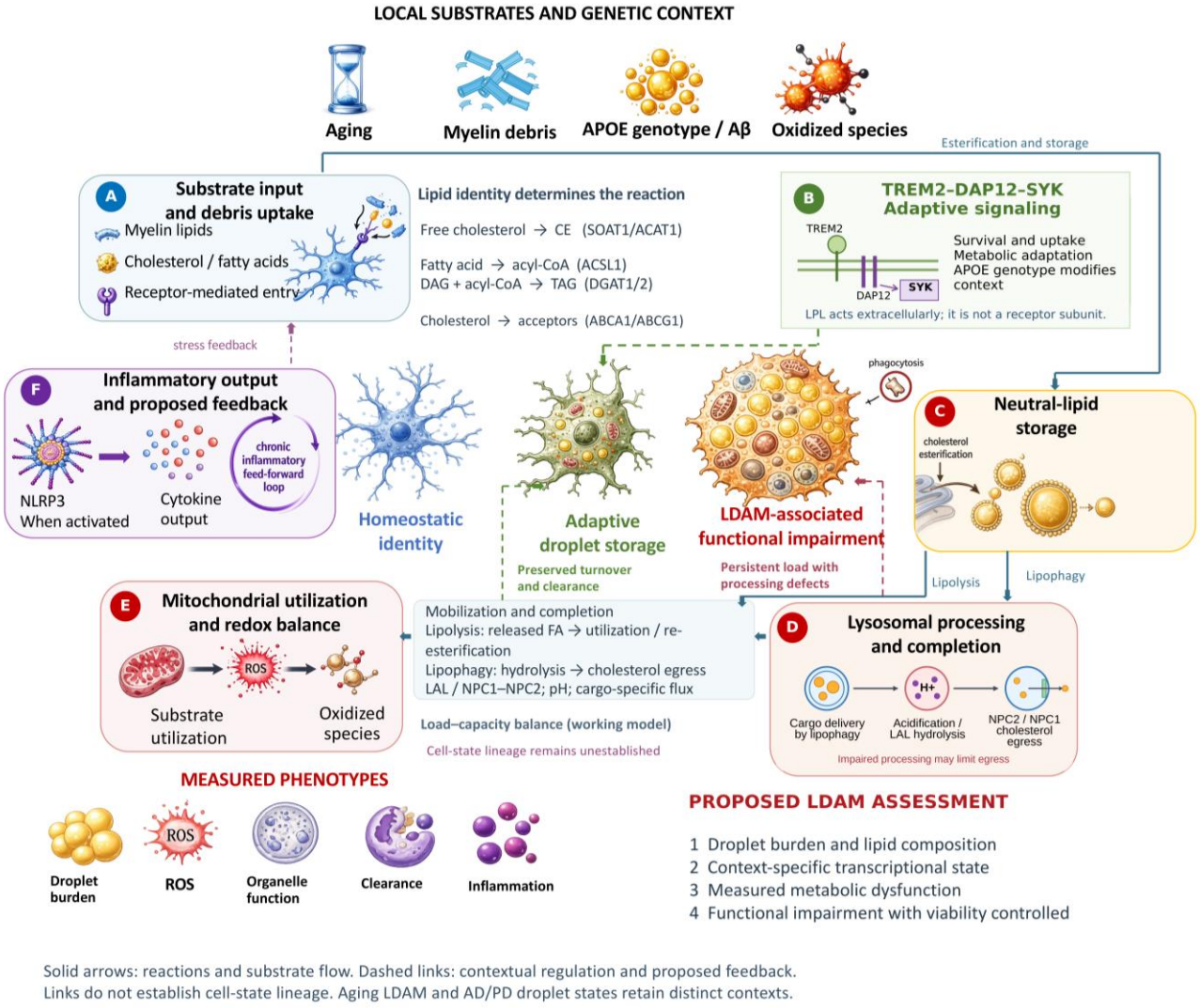


Figure 2. Lipid processing, organelle capacity and LDAM assessment. (A) Uptake and neutral-lipid synthesis, distinguishing SOAT1/ACAT1-mediated cholesterol esterification, ACSL1-mediated fatty-acid activation, DGAT1/2-mediated TAG synthesis, and ABCA1/ABCG1-associated cholesterol export. **(B)** TREM2–TYROBP/DAP12–SYK receptor signaling, with APOE context. LPL is a separate extracellular lipid-processing protein, not a subunit of the receptor complex. (**C)** Lipid-droplet storage and mobilization. (D) Lysosomal delivery, acidification, hydrolysis, and NPC1/NPC2-dependent cholesterol egress. **(E)** Mitochondrial utilization and redox balance. **(F)** Inflammatory output and conditional feedback. The central cells illustrate the functional conditions compared in the text. The proposed assessment framework records droplet burden, transcriptional characterization, metabolic function, and cellular performance separately, with viability controlled. Solid arrows identify substrate-processing routes; dashed links identify conditional regulation or proposed feedback. Abbreviations: Aβ, amyloid-β; ABCA1/ABCG1, ATP-binding cassette transporters A1/G1; ACSL1, acyl-CoA synthetase long-chain family member 1; APOE, apolipoprotein E; CE, cholesteryl ester; DAG, diacylglycerol; DAP12, DNAX-activating protein of 12 kDa, encoded by TYROBP; DGAT1/2, diacylglycerol acyltransferases 1/2; FA, fatty acid; LAL, lysosomal acid lipase; LDAM, **lipid-droplet-accumulating microglia**; LPL, lipoprotein lipase; NLRP3, NLR family pyrin domain-containing 3; NPC1/2, Niemann–Pick C1/C2 proteins; ROS, reactive oxygen species; SOAT1/ACAT1, sterol O-acyltransferase 1, historically termed acyl-CoA:cholesterol acyltransferase 1; SYK, spleen tyrosine kinase; TAG, triacylglycerol; TREM2, triggering receptor expressed on myeloid cells 2.

For example, the myelin-loading SOAT1 study measured both free cholesterol and cholesteryl esters, whereas the APOE4-associated PI3K study measured droplet and autophagy-associated changes without demonstrating increased autophagic flux [21, 22]. The DGAT2 study improved amyloid uptake ex vivo and used a degrader delivered intracerebroventricularly in vivo [23]. These experiments resolve different reactions and translational questions. We use substrate input and processing capacity to organize the comparison and propose a four-dimension reporting checklist. Disease-associated microglia (DAM) and white-matter-associated microglia (WAM) provide transcriptional and anatomical comparators; LDAM requires its own structural and functional characterization.

Figure 1 summarizes brain lipid sources and intercellular handling; Figure 2 connects storage and mobilization with organelle function; Figure 3 presents spatial and multi-omics approaches to biological validation; and Figure 4 organizes pharmacological evidence.

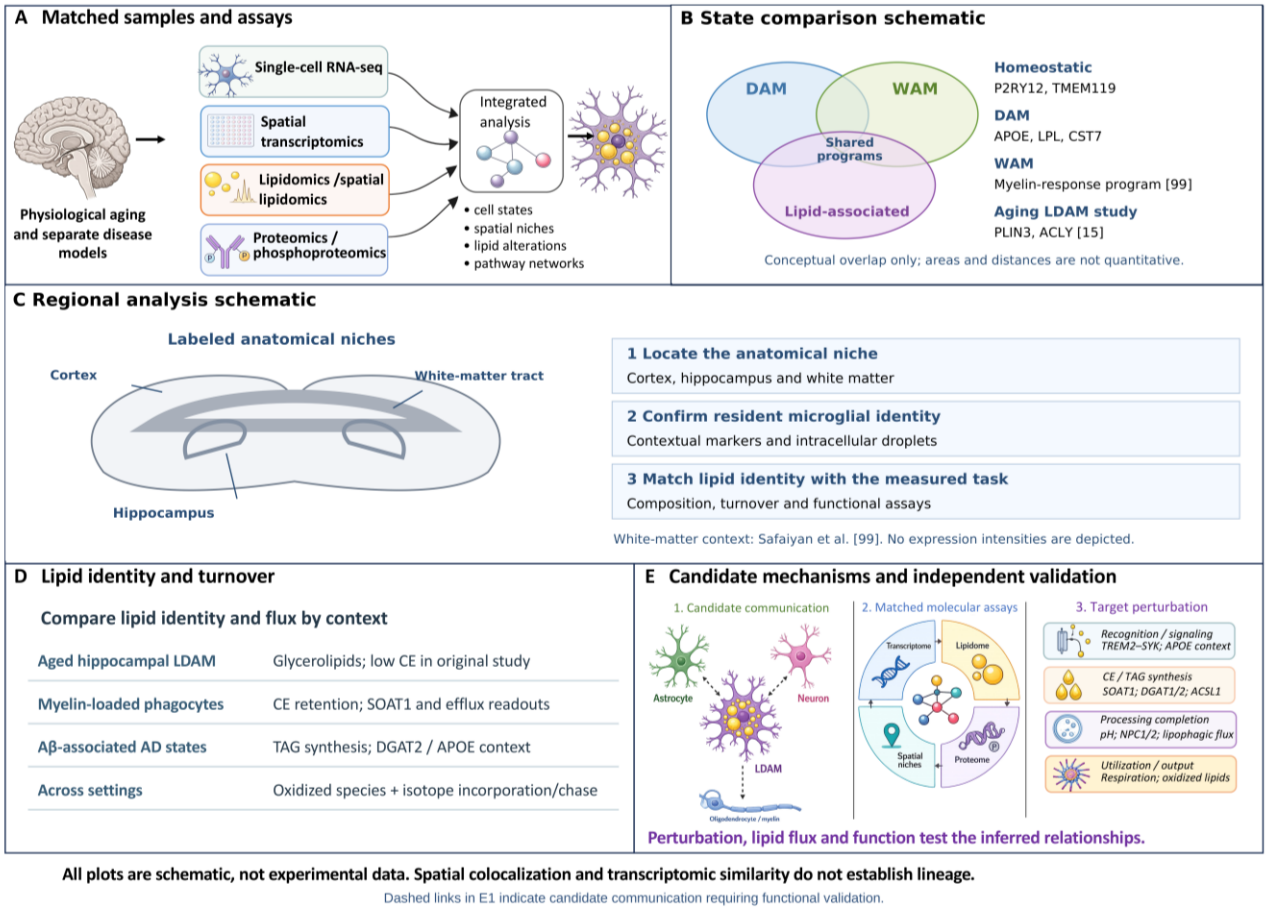


Figure 3. Spatial evidence and complementary measurements. **(A)** Integration of single-cell or single-nucleus transcriptomics, anatomical localization, lipidomics, and protein measurements. **(B)** Conceptual overlap of selected marker programs for homeostatic microglia, DAM, WAM, and lipid-associated populations; gene overlap is not a quantitative embedding. **(C)** Labeled anatomical niches for regional comparison, including hippocampal and white-matter contexts. **(D)** Comparison of lipid composition and direct turnover measurements. **(E)** Functional assays and target perturbations that test the candidate reaction. Arrows indicate analytical integration or validation steps. The panel is a conceptual scheme without simulated experimental points or spatial-expression intensities. Abbreviations: Aβ, amyloid-β; ACLY, ATP citrate lyase; AD, Alzheimer's disease; APOE, apolipoprotein E; CE, cholesteryl ester; CST7, cystatin F; DAM, disease-associated microglia; IFN, interferon; LDAM, lipid-droplet-accumulating microglia; LPL, lipoprotein lipase; PLIN3, perilipin 3; RNA-seq, RNA sequencing; TAG, triacylglycerol; TMEM119, transmembrane protein 119; WAM, white-matter-associated microglia.

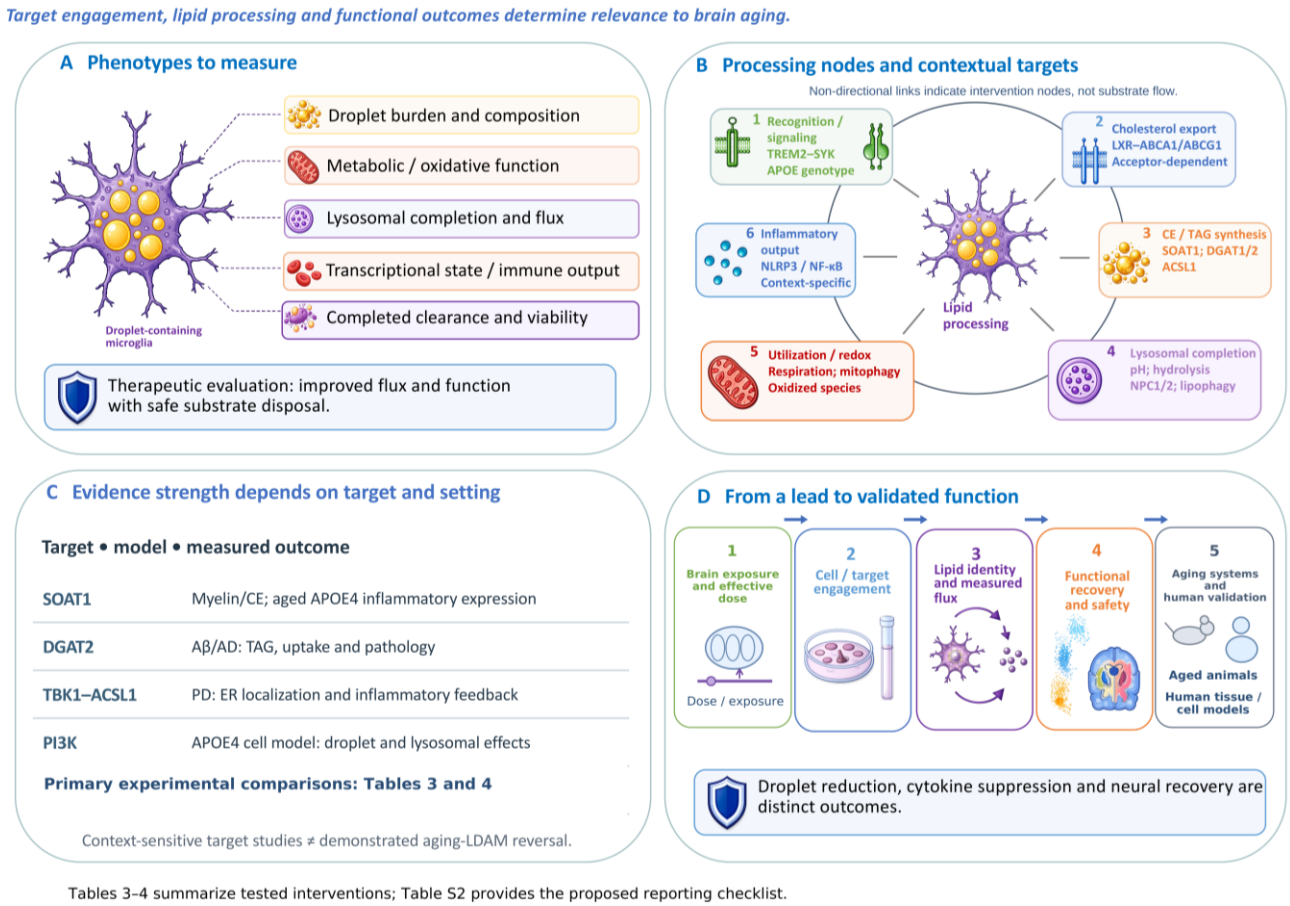


Figure 4. Pharmacological evidence and functional evaluation. **(A)** Complementary intervention endpoints: droplet burden and composition, substrate processing, cellular performance, inflammatory output, and viability. **(B)** Reactions and regulatory nodes evaluated in the text, including receptor signaling, cholesterol export, neutral-lipid synthesis, organelle processing, and redox control. **(C)** Tested SOAT1-, DGAT2-, TBK1–ACSL1-, and PI3K-associated interventions, distinguished by model, route, target validation, and measured outcome. **(D)** Proposed validation sequence: exposure and effective dose, cellular target engagement, the implicated lipid-processing reaction, functional recovery and safety, and confirmation in aging systems and human-derived models or tissue. Arrows indicate a research workflow. Abbreviations: Aβ, amyloid-β; ABCA1/ABCG1, ATP-binding cassette transporters A1/G1; ACSL1, acyl-CoA synthetase long-chain family member 1; AD, Alzheimer's disease; APOE, apolipoprotein E; CE, cholesteryl ester; DGAT1/2, diacylglycerol acyltransferases 1/2; ER, endoplasmic reticulum; LDAM, lipid droplet-accumulating microglia; LXR, liver X receptor; NF-κB, nuclear factor κB; NLRP3, NLR family pyrin domain-containing 3; NPC1/2, Niemann–Pick C1/C2 proteins; PD, Parkinson's disease; PI3K, phosphoinositide 3-kinase; SOAT1, sterol O-acyltransferase 1; SYK, spleen tyrosine kinase; TAG, triacylglycerol; TBK1, TANK-binding kinase 1; TREM2, triggering receptor expressed on myeloid cells 2. Shared interpretation note for Figures 1–4. The figures are conceptual illustrations. Cell-state overlap and anatomical proximity do not establish ancestry; the study-specific evidence supporting each pathway is described in the text and Tables 3–4. AI-assisted illustration preparation is described in the manuscript declaration.

1.1 Scope and evidence appraisal

This narrative synthesis considers English-language literature on brain aging, microglia, lipid metabolism, lipid droplets, APOE, TREM2, autophagy, mitochondria, and inflammatory signaling. A targeted literature update was completed on 27 October 2026 for the mechanistic and intervention comparisons. PubMed/Europe PMC records, primary articles, supplementary material, and cited correction notices were checked for the central studies. Primary studies in physiological aging provide the reference for aging-associated phenotypes. Disease-model and cell-culture findings retain their species, age, sex, region, genotype, substrate, intervention, and assay context. Tables 3 and 4 separate measured results from mechanistic interpretation and record assay-specific sample sizes rather than treating cells or image fields as independent animals. The four-dimension checklist in Supplementary Table S2 is a proposed reporting aid, not a validated diagnostic score. Transcriptional overlap, spatial proximity, and

disease-model findings do not establish population ancestry or equivalence to physiological-aging LDAM; these boundaries apply throughout the text and figures. This is a critical narrative review, without the completeness claims or formal evidence grading of a systematic review.

2. Lipid identity, storage, and flux in brain aging

Lipid remodeling in the aging brain involves synthesis, transport, storage, degradation, and oxidation [8, 9, 12, 18, 24]. Tissue lipidomics describes the substrate environment, although measured concentrations reflect several cell types and metabolic processes. Table 1 summarizes lipid classes and their relevance to microglial processing, and Figure 1 illustrates the cellular division of labor.

2.1 Lipid identity and biological effects

Cholesterol supports membrane organization, synapses, and myelin, with brain homeostasis relying largely on local synthesis and intercellular redistribution [7, 25-27]. Its aging-associated changes vary by cell and region [28, 29]. Free cholesterol and cholesteryl esters (CE) occupy different metabolic pools: SOAT1/ACAT1-mediated esterification moves cholesterol into neutral-lipid storage, while hydrolysis, intracellular trafficking, and export determine its subsequent fate. Myelin-clearance and chronic phagocytic-challenge studies identify cholesterol retention under high substrate demand [9, 14]. The glycerolipid-rich droplets of aged hippocampal microglia provide a different compositional reference [15]; Section 6 compares these findings quantitatively.

Table 1. Major brain lipid classes and their relevance to microglial processing.

Lipid class	Representative species	Physiological role	Aging-related context	Processing consequence	Relevance to LDAM
Cholesterol [7, 9, 14, 15, 22]	Free cholesterol; CE	Membranes, synapses, myelin	Transport and compartmentalization vary by cell and region	SOAT1 esterification buffers free cholesterol; retained CE can indicate poor mobilization/export	CE-rich myelin-loaded cells differ from glycerolipid-rich aging LDAM
Phospholipids [31, 33, 36, 37]	PC; PE; PS	Bilayer structure and vesicle trafficking	Remodeling, oxidation, or PS exposure	Changes membrane function and phagocytic substrates	Measure membrane species separately from droplet neutral lipids
Sphingolipids [8, 30, 32]	Ceramides; sphingomyelin; glycosphingolipids	Myelin, membrane domains, signaling	Species- and region-dependent remodeling	Particular ceramides influence stress signaling and mitochondrial function	Tissue abundance alone does not assign a microglial state
PUFA-containing lipids [37–43]	DHA; EPA; arachidonate-containing species	Membrane properties and lipid mediators	Unsaturation and oxidation depend on molecular pool	Peroxidized phospholipids differ from PUFA stored in TAG	Identify oxidized species and cellular compartment
Neutral lipids in droplets [14, 15, 23, 47, 102]	TAG; CE	Temporary substrate sequestration	Input, synthesis, mobilization, utilization, and export jointly determine storage	Rapid turnover can support adaptation; retention may accompany dysfunction	Droplets are organelles; burden is one of four assessment dimensions

CE, cholesteryl ester; TAG, triacylglycerol; PC, phosphatidylcholine; PE, phosphatidylethanolamine; PS, phosphatidylserine; PUFA, polyunsaturated fatty acid. Molecular species, compartment and experimental context determine interpretation.
Note. Each row cites the sources supporting its lipid class and cellular role. Molecular species, compartment, region, and experimental setting are retained when interpreting lipid measurements.
Abbreviations: CE, cholesteryl ester; DHA, docosahexaenoic acid; EPA, eicosapentaenoic acid; LDAM, **lipid-droplet-accumulating microglia**; PC, phosphatidylcholine; PE, phosphatidylethanolamine; PS, phosphatidylserine; PUFA, polyunsaturated fatty acid; SOAT1, sterol O-acyltransferase 1; TAG, triacylglycerol.

Sphingomyelin, glycosphingolipids, ceramides, and sphingosine-1-phosphate contribute to membrane domains, myelin, and stress signaling [30, 31]. Particular ceramides can disturb mitochondrial function, with effects depending on molecular species and cellular context [32]. Their relevance to microglial function therefore depends on where they accumulate and which organelle they affect. Tissue ceramide abundance describes part of the substrate environment but cannot identify the composition of an individual cell's droplets.

Phosphatidylcholine, phosphatidylethanolamine, and phosphatidylserine regulate membrane fluidity, curvature, and vesicle trafficking [33-35]. Remodeling, oxidation, and phosphatidylserine exposure change the substrates presented to microglial recognition systems [36, 37]. These events can increase processing demand or injure membranes independently of neutral-lipid storage. Distinguishing oxidized membrane phospholipids from lipids within the droplet core avoids attributing every form of lipid injury to droplets.

PUFAs such as DHA and EPA support membranes and pro-resolving mediators [38-40], and their remodeling influences neural and immune resilience during aging [41, 42]. Their susceptibility to peroxidation creates a competing source of injury [43]. Triacylglycerol (TAG) storage can sequester excess fatty acids, but its consequences depend on fatty-acid composition and the fate of substrates released during mobilization. PUFA-containing neutral lipids and peroxidized PUFA phospholipids occupy different pools. The latter are relevant to ferroptotic injury, whereas droplet staining reports neutral-lipid abundance without resolving either composition or oxidation.

2.2 Mechanisms of input, esterification, mobilization, and export

Lipid burden reflects input, synthesis, mobilization, and disposal. Increased uptake, restricted hydrolysis, and inadequate export can each enlarge storage [9, 14, 24]. The same morphological endpoint can therefore arise from different reactions. Figure 2 separates these routes so that a change in droplet abundance can be related to the step responsible for it.

2.2.1 SOAT1/ACAT1, ACSL1, and DGAT1/2

SREBP2–HMGCR regulates cholesterol synthesis. SOAT1 encodes the cholesterol-esterifying enzyme commonly called ACAT1, which transfers an acyl group from acyl-CoA to free cholesterol to form CE. **DGAT1/2 produces triacylglycerol** from diacylglycerol and acyl-CoA. ACSL1 activates long-chain fatty acids to acyl-CoA, which can enter storage, membrane synthesis, or oxidation [44-47]. These reactions are affected by age and cellular context [28, 29]. In female APOE4-targeted-replacement mice aged 16–20 months, daily intravenous nanoparticle-formulated F12511 for 13–14 days reduced forebrain TLR4 and selected inflammatory cytokines [48]. These bulk-tissue outcomes are distinguished from the primary-microglial lipid measurements and from direct metabolic-flux evidence in Section 8. Throughout this review, ACAT1 refers to the SOAT1 cholesterol acyltransferase, not mitochondrial acetyl-CoA acetyltransferase.

2.2.2 APOE lipoproteins and cholesterol efflux

APOE-containing lipoproteins redistribute cholesterol and phospholipids between cells, while ABCA1 and ABCG1 support cholesterol export to extracellular acceptors [7, 49, 50]. Myelin and cellular debris deliver a substantial cholesterol load to phagocytes [9, 51]. Successful disposal requires accessible intracellular cholesterol, competent transporters, and suitable acceptors. Transporter expression and exported cholesterol are thus related but different endpoints. Labeled-cholesterol release, together with free-cholesterol and CE measurements, can locate the export limitation.

2.2.3 Lipolysis, lipophagy, and cholesterol trafficking

Cytosolic lipolysis releases fatty acids from neutral lipids, while lipophagy delivers droplet material to lysosomes for hydrolysis. Lysosomal acid lipase releases cholesterol from CE, after which NPC1/NPC2-dependent trafficking makes cholesterol available for reuse or export. TFEB regulates the transcription of autophagy and lysosomal genes [52-54]. Aging-related lysosomal changes [55, 56] and microglial autophagy deficiency in disease models [57, 58] can restrict different steps in this route. Delivery, hydrolysis, cholesterol egress, and final export therefore require separate interpretation.

2.2.4 Oxidation, utilization, and peroxidation

Fatty acids released from droplets can enter mitochondrial oxidation, undergo re-esterification, or support membrane synthesis. Their fate depends on utilization and redox capacity [43, 59, 60]. Insufficient GPX4 defense increases susceptibility to iron-dependent phospholipid oxidation and ferroptosis [61-63]. These pathways motivate measuring free substrates and oxidized lipids alongside storage, as illustrated by the intervention comparisons in Section 8.

2.3 Cell origin and disease context

Lipid changes in aging and disease arise in different molecular and cellular settings [48, 64-68]. Region, cell origin, and isolation procedures influence the measured lipid profile. Aged microglia, myelin loading, AD, and PD provide distinct settings for comparing processing mechanisms; these comparisons are developed in Section 6.

2.3.1 Division of labor between neurons and glia

Neuronal cholesterol balance, astrocytic lipid metabolism, and oligodendrocyte/myelin turnover impose different demands on the aging brain [9, 29, 69, 70]. Direct neuron–astrocyte experiments demonstrate activity-induced transfer and buffering of potentially toxic fatty acids [71], while APOE4 glial models show cell- and donor-dependent cholesterol defects [72]. Microglia encounter the resulting extracellular cargo and contribute debris clearance and immune responses [10, 17]. Figure 1 summarizes this division of labor.

2.3.2 Boundaries of disease-derived evidence

APOE- and Aβ-associated lipid responses in AD [13, 21, 73, 74], α-synuclein- and ACSL1-related findings in PD [75-77], and lipid or oxidative abnormalities in ALS [78-80] provide complementary comparisons of substrate handling. Their distinct genetics, cell types, and assay endpoints are retained in Section 6 and Table 4.

Together, these differences place substrate supply and processing capacity at the center of microglial lipid responses.

3. Cellular and transcriptional context of microglial lipid responses

Microglial lipid handling reflects both cell-intrinsic regulation and the local environment [81-83]. Transcriptional programs identify how cells respond to these demands, while metabolic and functional measurements establish what they accomplish. The distinction is especially important when comparing states defined by different experimental systems.

3.1 Homeostatic identity and clearance tasks

P2RY12, TMEM119, CX3CR1, SALL1, and environmental signals such as TGF-β support microglial identity and surveillance [5, 84-86]. Aging studies reveal heterogeneous changes in surveillance, clearance, and inflammatory responses [81, 87]. Identity markers should therefore be interpreted in context, especially when activated resident microglia downregulate homeostatic genes. Lipid phenotyping requires an independent assessment of the intracellular droplets and the cellular task affected.

3.2 Uptake versus completed clearance

TREM2, CD36, and lipoprotein receptors contribute to recognition and uptake; APOE and LXR–ABCA1/ABCG1 support lipid redistribution and export [13, 14, 88, 89]. These processes can become uncoupled. An increase in intracellular cargo may reflect more entry, slower processing, or both. Uptake followed by a chase period, with measurements of degradation products and cargo disappearance, distinguishes these possibilities and connects receptor activity to tissue clearance.

3.3 Astrocyte–microglia interactions

Astrocytic APOE lipoprotein supply and fatty-acid buffering interact with microglial debris processing [7, 71]. Inflammation, complement, and specific toxic lipids can further affect neighboring cells [90-92]. Intercellular lipid transfer provides a metabolic basis for these interactions and can be examined through labeled substrates and cell-specific perturbations.

3.4 Functional validation of immunometabolic remodeling

Microglial glycolysis, oxidative phosphorylation, and fatty-acid utilization vary with stimulus and disease setting [93-96]. Increased storage may accompany adaptation to energetic demand or an inability to use the incoming substrate. Metabolic gene expression alone cannot distinguish these outcomes. Respiration, ATP production, and substrate tracing, interpreted alongside viability, can identify whether the limiting reaction lies in energy supply or lipid disposal.

3.5 Relationships among DAM, WAM, and LDAM

Single-cell studies distinguish homeostatic, disease-associated, interferon-responsive, and inflammatory microglial programs [97, 98]. DAM were defined in neurodegenerative models and show reduced homeostatic genes with changes in APOE, LPL, CST7, TYROBP, or ITGAX [13, 74]. Safaiyan and colleagues defined WAM by profiling white and gray matter separately: the white-matter population expressed phagocytic and lipid-metabolism programs and accumulated with aging [99]. In that study, aging-associated WAM required TREM2 but formed independently of APOE, whereas their premature appearance in an AD model was APOE-dependent. This context dependence makes anatomical origin and experimental setting essential when comparing partially overlapping signatures.

The original LDAM work links droplet accumulation to oxidative and phagocytic abnormalities, while subsequent literature places these findings within broader aging and disease responses [15, 16]. Droplet-associated dysfunction therefore requires functional characterization in addition to cell-state markers. Section 6 develops this assessment and compares the evidence across experimental contexts.

TREM2-associated DAM responses can support injury processing, while interferon-responsive programs occur in aging white matter [6, 13, 97, 100]. Marker overlap identifies shared response components. The experiments required to test population ancestry are considered together in Section 6.6.

Table 2 compares states by their defining context. Figure 2 relates receptor signaling and lipid processing to the cellular tasks evaluated experimentally.

4. Mechanisms linking lipid processing to microglial function

4.1 Cholesterol input and limiting disposal reactions

Age-related myelin fragmentation progressively increases the lipid cargo taken up by microglia. Safaiyan and colleagues showed myelin-derived material accumulating in microglial lysosomal compartments during aging [101]. Subsequent work linked defective cholesterol clearance to impaired remyelination in the aged central nervous system [9]. These studies place substrate input and lysosomal storage within an anatomical and age-defined process rather than inferring them from transcription alone. An informative counterexample comes from focal demyelination in young adult male mice: loss of TREM2 or SOAT1 reduced adaptive lipid-droplet formation and was associated with unresolved phagocyte responses and impaired repair [102]. Thus, less storage and better tissue recovery are experimentally separable outcomes. The intervention question is which reaction limits safe processing in the population being studied.

Table 2. Microglial response states and proposed assessment of LDAM.

State / context	Representative features	Functional interpretation	Lipid-related measurements	Relationship to aging LDAM
Homeostatic [5, 84–86]	P2RY12; TMEM119; CX3CR1; SALL1	Surveillance and routine clearance	Uptake, processing, and export when measured	Reference identity; marker loss alone does not diagnose LDAM
DAM: disease-defined [13, 74]	APOE; LPL; CST7; TYROBP; ITGAX; altered homeostatic genes	Damage response can include adaptive clearance	Substrate handling depends on disease and TREM2 function	Shared genes do not establish LDAM ancestry
WAM: white-matter-associated [99]	White-matter enrichment; phagocytic and myelin-processing programs	TREM2-dependent in aging; APOE-independent in aging, APOE-dependent in AD	Pair anatomical identity with myelin and lipid assays	Anatomical program; lineage remains untested
IFN-responsive /inflammatory [100]	ISG15; IFIT genes; STAT1, or cytokine programs	Stimulus-dependent immune response	Metabolic demand requires direct measurement	Neither cytokines nor CD68/LAMP1 alone identify LDAM
Aging LDAM: joint assessment [15, 124, 125]	Droplet burden + transcription + metabolism + function	Original aged-mouse work: impaired phagocytosis, ROS and inflammatory output	Quantify burden/composition; multigene state; turnover/efflux; completed clearance	Four proposed reporting dimensions; no validated score or universal single-gene cutoff
Disease-associated droplet states [21, 23, 77]	APOE4/AD ACSL1; Aβ–DGAT2; PD TBK1–ACSL1	Functions depend on genotype, substrate, and model	Retain each measured dimension and unmeasured endpoint	Compare with aging LDAM without assuming equivalence

Markers retain their study-specific definitions. The proposed reporting checklist is provided in Table S2; Table 4 records the dimensions measured in each primary study.
Note. Markers describe context-specific programs. The original aging-LDAM report and each disease-associated comparison retain their experimental definitions. Supplementary Table S2 supplies the proposed reporting checklist; Table 4 records which dimensions were measured.
Abbreviations: Aβ, amyloid-β; ACLY, ATP citrate lyase; ACSL1, acyl-CoA synthetase long-chain family member 1; AD, Alzheimer's disease; APOE, apolipoprotein E; DAM, disease-associated microglia; DGAT2, diacylglycerol acyltransferase 2; IFN, interferon; LDAM, lipid-droplet-accumulating microglia; PD, Parkinson's disease; PLIN3, perilipin 3; ROS, reactive oxygen species; TBK1, TANK-binding kinase 1; TREM2, triggering receptor expressed on myeloid cells 2; WAM, white-matter-associated microglia.

4.2 TREM2–TYROBP/DAP12–SYK and APOE genotype

TREM2 signals through TYROBP/DAP12 and SYK to support survival, phagocytosis, and metabolic adaptation, while APOE contributes to lipid transport and transcriptional responses [13, 74, 89, 103]. TREM2 function cannot be reduced to promoting droplet formation: its loss worsens cholesterol-handling defects and CE accumulation during chronic phagocytic challenge [14]. Conversely, reduced plaque-associated lipid staining in human TREM2-R47H microglia in a chimeric AD model accompanied reduced plaque engagement; fewer PLIN2-positive structures did not demonstrate improved lipid disposal [104]. Human APOE4 microglial studies add distinct functional observations, including impaired surveillance of

neuronal-network activity [105] and donor-dependent cholesterol/lysosomal changes [72]. SYK deletion further separates plaque-associated responses from TREM2-linked DAP10 contributions to proliferation and an early DAM program [106]. These findings distinguish receptor competence, APOE context, and downstream substrate processing.

4.3 Droplet composition and organelle coupling

Droplets arise from the endoplasmic reticulum and contain a neutral-lipid core, a phospholipid monolayer, and associated proteins [47, 107]. Contacts with mitochondria and lysosomes connect storage to substrate release and utilization. CE/TAG proportions, acyl-chain composition, and organelle capacity can therefore change the outcome of a similar droplet burden. Myelin-processing, lipophagy, and AD autophagy-deficiency studies resolve different parts of this relationship [22, 54, 58]. The comparison is most informative when the lipid measured and the reaction perturbed are identified together.

The myelin-loading and Aβ studies illustrate different biochemical responses. In HMC3 cells exposed to myelin debris for 24 h, CE mass rose by 125%, free cholesterol by 180%, and TAG by 150%. F12511 reduced CE by 50% and free cholesterol by 51% in the loaded cells, while TAG was not significantly changed; K604 reduced labeled-oleate incorporation into CE by approximately 87% [22]. The measured tracer endpoint was ester synthesis, and ABCA1 induction supported an export-related mechanism without directly quantifying net cholesterol efflux. By contrast, the Aβ–DGAT2 study identified lower free fatty acids with higher TAG and showed that DGAT2 inhibition reduced droplet burden and improved amyloid uptake in selected microglia [23]. The distinction between cholesterol handling and fatty-acid esterification therefore changes both the target and the readout needed to judge benefit.

4.4 Engulfment, acidification, and completed degradation

Phagocytosis includes recognition, internalization, phagolysosomal processing, and disposal of degradation products [108, 109]. Droplet-associated phagocytic defects in aging and autophagy abnormalities in AD models can interrupt different steps [15, 58]. A cell may retain uptake but lose hydrolytic capacity, or exhibit reduced uptake despite relatively intact lysosomes. pHrodo signal primarily indicates delivery to an acidic compartment. Pairing it with proteolysis and cargo disappearance during a chase period can identify whether the defect precedes or follows acidification.

4.5 Sources and limits of inflammatory feedback

Cholesterol-crystal and efflux-defect studies in peripheral macrophages establish routes from lipid handling to inflammasome activation [110-112]. Their application to microglia depends on the presence of the same substrates and activation conditions. A droplet-associated inflammatory phenotype could reflect a toxic lipid pool, organelle injury, or an inflammatory signal that also induces storage. Reaction-specific perturbation, with lipid and functional readouts, is needed to distinguish these explanations. The inflammatory and organelle mechanisms are examined below.

4.6 LDAM and senescence-like phenotypes

Senescence-associated glial lipid accumulation provides a related comparison [113, 114], while reviews distinguish senescent microglia from other damage-associated populations [115, 116]. p16/p21 expression, inflammatory secretion, and lipid storage describe different processes. Their co-occurrence should be assessed with persistent damage, cell-cycle and lysosomal phenotypes, and cellular performance rather than using any single marker as a senescence label.

The consequence of a storage response depends on the organelles that receive mobilized lipids and complete cargo processing.

5. Organelle processing capacity and inflammatory output

Mitochondria, lysosomes, and redox systems jointly support adaptation to lipid stress [1, 10, 93]. Utilization of released substrates, completion of lysosomal hydrolysis, and repair of oxidative damage determine whether a given lipid input expands the cellular burden.

5.1 Chronic inflammation and lipid processing

Age-associated inflammation and local tissue injury can alter microglial uptake and metabolic demand [6, 11, 83, 117]. In turn, retained cargo and damaged organelles may prolong inflammatory signaling. This reciprocal regulation can maintain dysfunction after the initial substrate challenge. Changes in cytokines and changes in lipid turnover need to be measured together to determine whether an intervention interrupts the metabolic restriction, its inflammatory consequence, or both.

5.2 NLRP3 and inflammatory amplification

Cholesterol crystals, organelle injury, and mitochondrial danger signals can activate NLRP3 in peripheral macrophages and neurological-disease models [111, 118].

Elevated ROS and inflammatory output in aging LDAM make this a plausible amplification mechanism [15, 16], but the original droplet phenotype does not establish a universal NLRP3-dependent state. ASC assembly, caspase-1 processing, and mature IL-1β or IL-18 identify inflammasome activity. Cell-specific perturbation can then determine whether that activity contributes to defective clearance or primarily to inflammatory output.

5.3 Compartments of ROS and lipid peroxidation

Aged LDAM showed increased CellROX signal and an exaggerated cytokine response to LPS [15]. These observations concern cellular redox state and inflammatory reactivity. Mitochondrial ROS, oxidized membrane phospholipids, and neutral-lipid oxidation are distinguishable measurements [59, 60, 119], and locating the affected compartment helps connect the oxidative phenotype to a particular processing defect.

5.4 Matching mitochondrial utilization to lipid mobilization

Mitochondrial quality control and metabolic adaptation influence microglial inflammatory responses [59, 93]. Droplet–mitochondrial contacts connect stored substrates to utilization, although the fate of released fatty acids depends on demand and enzyme activity [16, 47]. If oxidation is limiting, faster mobilization can increase substrate delivery without increasing consumption. The predicted consequence is redistribution into free fatty acids, re-esterified lipids, or oxidized products. Measuring these pools alongside respiration tests whether lower TAG reflects improved use or movement of the burden elsewhere.

5.5 Autophagosome formation, flux, and lysosomal completion

Autophagy and mitochondrial quality-control studies in disease models link organelle processing to lipid retention and inflammation [56, 58, 120, 121]. These processes contain several separable steps: autophagosome formation, fusion and cargo delivery, lysosomal acidification and hydrolysis, and trafficking of released products. LC3-II or p62 accumulation can accompany either increased formation or restricted degradation. Similarly, CD68 and LAMP1 indicate organelle-associated abundance rather than completed clearance. Turnover measurements with lysosomal blockade, tandem reporters, and cargo-chase assays resolve this ambiguity [122]. TFEB localization reports transcriptional regulation; lysosomal pH and proteolysis report processing capacity; NPC1/NPC2-dependent egress reports cholesterol trafficking. Lipophagy and mitophagy concern different cargoes and should be assessed accordingly.

5.6 Ferroptosis and cell identity

Insufficient GPX4-related defense permits iron-dependent phospholipid peroxidation and ferroptosis [63]. Direct neuronal evidence includes forebrain-neuron Gpx4 ablation, which caused neurodegeneration and cognitive impairment, and motor-neuron ferroptosis experiments in ALS models [80, 123]. These studies establish neuronal susceptibility in their respective systems. A corresponding claim in aging microglia would require cell-resolved lipid peroxidation, cell-death measurements, and rescue by iron chelation or ferroptosis inhibition. ROS production by viable droplet-containing microglia is a separate phenotype.

The model therefore allows several origins of impaired processing: excessive substrate input, restricted degradation or export, inadequate utilization, or increased inflammatory demand. These restrictions can reinforce one another. Their relative contribution, rather than a presumed stage, determines which reaction offers a rational intervention point.

In Figure 2, solid arrows identify substrate-processing routes and dashed links identify conditional regulation or proposed feedback. The cells summarize the functional conditions compared in the text.

6. Defining LDAM and comparing droplet-associated states

6.1 Direct evidence in physiological aging

Marschallinger and colleagues studied young and aged male C57BL/6J mice, using mainly 2–4- versus 18–20-month-old animals. In hippocampal dentate gyrus, BODIPY-positive TMEM119-positive microglia increased from 12.08% in young mice to 51.95% in aged mice (n = 6 mice per group). Label-free coherent anti-Stokes Raman scattering independently detected lipid-rich microglia in 18.93% versus 50.76%, respectively (n = 5 per group). Isolated droplets from aged microglia contained 44.4% glycerolipids and 0.7% CE (n = 4 mice per group for the reported lipidomic experiment) [15, 124, 125]. These assay-specific values describe both the magnitude of the aging phenotype and its predominantly glycerolipid-rich composition.

The same study linked high droplet burden to reduced zymosan and labeled-myelin uptake, increased ROS, and heightened cytokine release. Transcriptomic comparisons identified 692 differentially expressed genes, including PLIN3, ACLY, CD63, and trafficking-associated genes [15]. Human hippocampal observations were histological,

with PLIN2-positive IBA1-positive cells, rather than direct tests of metabolic turnover or phagocytic performance. Independent aging studies broaden the comparison: Shimabukuro and colleagues found regionally heterogeneous lipid-laden cell types in female mice aged 18–22 months, including several non-microglial populations [126]; Arbaizar-Rovirosa and colleagues linked age-associated microglial lipid loading to an impaired response to ischemic injury [127]. These results support an age-related phenotype while showing why cell identity, anatomical niche, and measured function need to be reported alongside staining. A recent neuronal Pla2g2f study further links an aging-induced extracellular signal to microglial lipid handling and hippocampal-cortical resilience [128].

6.2 Candidate mechanisms and unresolved state origin

The foundational LDAM study also tested mechanisms. A BV2 CRISPR–Cas9 screen targeting approximately 2,000 lysosomal, protein-degradation, and stress-response genes identified 112 regulators of lipid-droplet formation using the corrected significance criterion ($P < 0.05$; false discovery rate < 5%) [15, 124]. Individual perturbations implicated GRN, SLC33A1, VPS35, and SNX17. Male Grn-null mice at 9–10 months had approximately twice the proportion of droplet-positive microglia and twice as many droplets per cell as wild-type littermates, with associated uptake and inflammatory abnormalities [15]. These genetic findings connect lipid storage to lysosomal and trafficking biology. Brain-penetrant progranulin delivery subsequently rescued lysosomal-storage phenotypes in Grn-deficient mice [129, 130], providing a mechanistic comparison rather than evidence that normal aging LDAM had been reversed.

LPS exposure also induced lipid droplets in young mice and in BV2 cells in the foundational study [15]. This supports an inflammatory route to a similar structural phenotype, alongside the genetic and substrate-loading routes. The triacsin C experiments and their causal limits are discussed in Section 6.4 and Table 3.

Table 3. Tested interventions and their measured outcomes.

Study and setting	Intervention and exposure	Target and delivery evidence	Measured outcomes	Scope and limitations
SOAT1 and myelin loading Huynh et al. 2024 [22]	HMC3 and N9 cells; myelin debris for 24 h. K604 or F12511, 0.5 μM for 24 h. GSK2033, 5 μM, tested LXR dependence.	CE-synthesis inhibition with two compounds. K604 is SOAT1-selective; F12511 also inhibits SOAT2. GSK2033 blocked ABCA1 induction. Cell-culture experiment; brain exposure not tested.	In HMC3, K604 reduced labeled-oleate incorporation into CE by about 87%. F12511 reduced CE mass by 50% and free cholesterol by 51% in myelin-loaded cells; TAG was not significantly changed. ABCA1 increased.	Tracer incorporation measures synthesis. Net cholesterol efflux, completed cargo degradation, and aging-brain functional recovery were not directly established.
SOAT1 and APOE4 aging Huynh et al. 2024 [48]	Female APOE-targeted-replacement mice, 9 or 16–20 months. Nanoparticle F12511, 46 mg/kg daily for 13–14 days, alternating tail-vein and retro-orbital venous administration.	Systemic administration with bulk-forebrain pharmacodynamic readouts. Primary APOE4 microglial experiments supported a lipid and ABCA1 response. Microglial drug concentration and cell-resolved in vivo engagement were not quantified.	In 16–20-month animals, forebrain TLR4 and selected cytokines decreased. Bulk ABCA1 was unchanged; PLIN2 showed a decreasing trend. Cellular and in vivo outcomes are kept separate.	No direct measurement of microglial turnover, completed clearance, or cognitive recovery. Nanoparticle/vehicle effects and F12511 isoform selectivity limit target attribution.
DGAT2 inhibition ex vivo Prakash et al. 2025 [23]	Microglia from 5–7-month female WT and 5xFAD mice. D2i (Sigma PZ0233), 15 μM, 1-h pretreatment, then 30-min Aβ-pHrodo exposure; drug maintained during staining.	Chemical inhibition supported by complementary Dgat2 genetic perturbation and a separate degrader arm. Direct exposure of isolated cells; brain delivery not tested in this arm.	Droplets decreased by 51% in WT and 57% in 5xFAD-derived microglia. Aβ-pHrodo uptake in droplet-positive 5xFAD microglia increased 1.41-fold.	The uptake assay includes acidified-compartment delivery, not a completed-degradation chase. The inhibitor and in vivo degrader are distinct interventions.

DGAT2 degradation in vivo Prakash et al. 2025 [23]	11–24-month 5xFAD mice. In-house DGAT2 degrader, 120 µM infusate at 1 µL/h into a lateral ventricle for 7 days.	Microglial DGAT2 protein volume decreased by about 55%, supporting engagement after local administration. Intracerebroventricular delivery bypasses systemic BBB entry.	Subicular plaque burden decreased by about 51%; plaque-proximal microglial droplet load by 40%; neuritic dystrophy by 47%. Effects are the article's reported treatment comparisons.	Does not establish systemic brain penetration, microglia-exclusive drug action, or efficacy in physiological aging without amyloid pathology.
TBK1–ACSL1 Han et al. 2025 [77]	BV2 cells exposed to LPS, 1 µg/mL for 12 h; GSK8612, 5 µM for 6 h. ACSL1/TBK1 knockdown and kinase-inactive TBK1 were complementary perturbations.	Reduced TBK1 Ser172 phosphorylation, interaction/localization studies, and Nrdp1/K63-ubiquitination experiments support the signaling mechanism. The principal GSK8612 experiment was cellular.	Droplet and inflammatory readouts decreased. Figure 6 reports three independent experiments; effect sizes are shown graphically rather than as numerical percentage summaries.	Total TBK1 reduction and kinase inhibition had distinct localization effects. The separate in vivo arm is recorded below; no completed-clearance rescue in aged microglia was tested.
TBK1 inhibition in vivo Han et al. 2025 [77]	Male C57BL/6 mice, 6–8 weeks, with LPS or MPTP models. GSK8612: 10 mg/kg/day for 7 days in the LPS timeline; 10 mg/kg/day intraperitoneally from day 0 to day 14 in the MPTP timeline. The main LPS timeline did not specify the drug-administration route.	Lower p-TBK1 in substantia-nigra tissue and reduced ER-ACSL1 in sorted microglia support a pharmacodynamic response. Brain drug concentrations, unbound exposure, and microglia-exclusive action were not measured.	Reduced IBA1 inflammatory response and TH-positive cell loss; reduced PLIN3 in the LPS arm. Selected motor outcomes improved. Histology n = 5 mice/group; ER-ACSL1 and immunoblots n = 3/group. Effects are plotted rather than numerically tabulated.	The MPTP dopamine comparison ($P = 0.0655$) and LPS pole test ($P = 0.0574$) were not significant. These young-animal PD models did not test aging-LDAM turnover or completed disposal.
PI3K-associated intervention Haney et al. 2024 [21]	APOE4/4 iPSC-derived microglia with fibrillar Aβ. GNE-317, 10 µM for 24 h. A CRISPR screen identified PIK3CA as a modifier of droplet accumulation.	Genetic screening and chemical response support PI3K-associated regulation. The tested compound has pathway-level activity; a response does not isolate one molecular target. Brain exposure was not measured in this cell experiment.	Droplet/PLIN2 and lysosomal accumulation and inflammatory secretion decreased. LC3B and autophagy-related expression changed.	The authors explicitly state that these observations do not establish increased autophagic flux. No in vivo aging-LDAM treatment or functional recovery trial was performed.
Long-chain acyl-CoA synthesis Marschallinger et al. 2020 [15, 124, 125]	BV2 cells: triacsin C, 1 µM, 30 min before LPS, 5 µg/mL; co-treatment for 18 h.	Broad long-chain acyl-CoA synthetase inhibition changes the supply of activated fatty acids for several pathways. This is not a droplet-specific manipulation.	LPS-induced droplets and ROS decreased; zymosan uptake increased. The genetic screen and Grn-null phenotypes supplied separate mechanistic evidence.	Does not distinguish a storage-specific effect from broader lipid-synthesis changes or demonstrate restored flux in naturally aged microglia.

Note. Regimens describe the cited experiments, not recommended treatment. Percentages are reported comparisons within each study. Target engagement, brain delivery, lipid processing and functional recovery are separate evidence fields. An unmeasured endpoint remains unknown.
Study-level age, sex, brain-region and assay-specific replication details are given in Table 4; unreported treatment-specific details are not inferred. Tracer incorporation measures synthesis, whereas lipid staining and ABCA1/PLIN expression do not establish turnover.
Note. Doses and durations describe the cited experiment, not a recommended regimen. Target validation, delivery, lipid endpoints, and functional outcomes are separate evidence fields. Brain-directed infusion does not establish systemic brain penetration. ACAT1 denotes SOAT1; F12511 also inhibits SOAT2.
Study-level age, sex, brain-region and assay-specific replication details are given in Table 4; unreported treatment-specific details are not inferred. Tracer incorporation measures synthesis, whereas lipid staining and ABCA1/PLIN expression do not establish turnover.
Abbreviations: Aβ, amyloid-β; ABCA1/ABCG1, ATP-binding cassette transporters A1/G1; ACSL1, acyl-CoA synthetase long-chain family member 1; AD, Alzheimer's disease; APOE, apolipoprotein E; ASC, apoptosis-associated speck-like protein containing a caspase recruitment domain; CE, cholesteryl ester; CoA, coenzyme A; DAG, diacylglycerol; DAP12, DNAX-activating protein of 12 kDa, encoded by TYROBP; DGAT1/2, diacylglycerol acyltransferases 1/2; FA, fatty acid; LAL, lysosomal acid lipase; LDAM, lipid-droplet-accumulating microglia; LXR, liver X receptor; NLRP3, NLR family pyrin domain-containing 3; NPC1/2, Niemann–Pick C1/C2 proteins; PD, Parkinson's disease; ROS, reactive oxygen species; SOAT1, sterol O-acyltransferase 1; SYK, spleen tyrosine kinase; TAG, triacylglycerol; TBK1, TANK-binding kinase 1; TFEB, transcription factor EB; TREM2, triggering receptor expressed on myeloid cells 2.

6.3 Four complementary dimensions of assessment

We propose four complementary reporting dimensions: droplet burden, transcriptional state, metabolic function, and cellular performance. Cell identity is a prerequisite, not an inference from lipid staining: resident microglia must be distinguished from infiltrating or border-associated macrophages using contextual markers, anatomy, and, where feasible, lineage information. Droplet burden is measured within identified cells, with counts or volumes and an orthogonal neutral-lipid or perilipin readout. Transcriptional characterization reports a context-appropriate multigene profile; PLIN2 or a single reactive marker is insufficient [131]. A metabolic defect requires a functional measurement of the implicated reaction, such as impaired substrate turnover, cholesterol efflux, lysosomal hydrolysis/egress, or utilization. Cellular impairment requires a relevant task deficit or injurious output with viability controlled. A pHrodo assay measures delivery into an acidic compartment and should be distinguished from completed degradation. Each assay should state its biological replication, matched comparator, and limitations. Supplementary Table S2 specifies minimum observations, suitable methods, and the inferences each can support. These are proposed reporting requirements, without a validated universal cutoff or additive diagnostic score.

Detection methods require their own controls. BODIPY/LipidTOX, Oil Red O, perilipin immunostaining, electron microscopy, and label-free Raman methods differ in sensitivity and in what they identify. Fixation, lipid extraction during paraffin processing, autofluorescence, tissue thickness, and segmentation can alter counts or apparent size. Matching acquisition and processing, confirming intracellular localization, and using an orthogonal readout improve comparability; quantitative BODIPY workflows provide a practical example [132].

6.4 Inflammatory associations and causal attribution

In LPS-stimulated BV2 cells, triacsin C at 1 μM, added 30 min before 5 μg/mL LPS and maintained for 18 h, suppressed droplet formation and ROS and increased zymosan uptake [15]. This is direct pharmacological evidence that perturbing lipid synthesis changes a microglial phenotype, but long-chain acyl-CoA synthetase inhibition also alters substrate availability for several metabolic pathways. The experiment therefore does not isolate a droplet-specific causal effect or demonstrate restored turnover in naturally aged microglia. The proposed checklist records that distinction without discarding the intervention result.

6.5 Distinct evidence from AD, PD, and ALS

Human APOE4/4 AD tissue and corresponding induced-microglial models identify an ACSL1-associated lipid phenotype, while conditioned medium from lipid-loaded cells induces neuronal tau phosphorylation and toxicity [21]. Other APOE4 models link lipid accumulation to impaired surveillance of neuronal-network activity [105] or lysosomal cholesterol sequestration with substantial donor-dependent variation [72]. These comparisons connect lipid measurements to different cellular tasks rather than assigning all APOE4-associated phenotypes to one processing defect.

In the Aβ–DGAT2 study, 15 μM DGAT2 inhibitor reduced droplets by 51% in wild-type and 57% in 5xFAD-derived microglia ex vivo. Amyloid uptake by droplet-positive 5xFAD microglia increased 1.41-fold. A seven-day intracerebroventricular DGAT2-degrader infusion in 11–24-month-old 5xFAD mice reduced subicular plaque burden by approximately 51%, plaque-proximal microglial droplet load by 40%, microglial DGAT2 protein volume by 55%, and neuritic dystrophy by 47% [23]. These are disease-model effects with distinct cellular and tissue endpoints. ALS lipidomics and motor-neuron ferroptosis studies provide additional comparisons, retaining their original cellular attribution [78-80]. Table 4 identifies which assessment dimensions were actually measured.

The PD TBK1–ACSL1 study combined human substantia-nigra datasets with LPS-, MPTP-, and α-synuclein-related experimental systems. In BV2 cells, 5 μM GSK8612 for 6 h during LPS exposure reduced TBK1 Ser172 phosphorylation, droplet accumulation, and inflammatory readouts; the key figure reports three independent experiments [77]. ACSL1 and TBK1 knockdown, kinase-inactive TBK1, interaction/localization assays, and ubiquitination experiments support a feedback mechanism involving ACSL1 redistribution to the endoplasmic reticulum, Nrdp1-mediated K63 ubiquitination of TBK1, and NF-κB-dependent ACSL1 expression. These interventions distinguish kinase activity from total TBK1 abundance. The in vivo drug results are discussed in Section 8.3; quantitative brain exposure and recovery of aging-associated clearance were not measured. PD also involves lipid-processing routes outside this circuit: GBA1-related glucosylceramide/lysosomal dysfunction participates in a bidirectional relationship with α-synuclein [133], and LRRK2 regulates lysosomal tubulation and vesicle sorting [134]. Those neuronal and cellular findings extend the mechanistic context without assigning all PD lipid abnormalities to microglial droplets.

6.6 State origin and lineage

Whether DAM or WAM contribute to LDAM remains an experimental question. A change in the abundance of transcriptional populations can reflect state conversion, selective survival, recruitment, or replacement. Inducible population labeling and serial measurements are needed to distinguish these explanations and to test whether the original lipid-loaded cells recover after intervention. Transcriptomic similarity, pseudotime, and spatial proximity can prioritize such experiments, but cannot establish ancestry. This restriction applies to all state comparisons and schematic figures in the review.

6.7 Functional recovery and cross-context comparison

Functional recovery requires improvement in the task impaired at baseline; a reduction in lipid droplets alone establishes neither improved lipid metabolism nor restored microglial function. Improved uptake, lysosomal processing, substrate export, and tissue repair are recorded as separate outcomes in Table 3. Their dissociation is informative: adaptive storage supported remyelination in the TREM2/SOAT1 study [102], whereas DGAT2 inhibition improved amyloid uptake and local brain infusion reduced pathology in a 5xFAD setting [23]. These observations support selecting interventions by substrate and limiting reaction rather than by the direction of the staining change alone.

For partially characterized populations, the measured dimensions should be named explicitly. Histological lipid-positive microglia are described as droplet-containing microglia; a transcriptomic match adds a stated lipid-associated program. Human postmortem tissue can support these structural and transcriptional observations, but usually cannot establish in vivo flux or recovery of a cellular task. Unmeasured metabolic or functional dimensions remain unknown, not normal and not impaired. Historical LDAM terminology is retained when discussing the original reports, with evidence coverage shown separately in Table 4.

Table 4. Primary studies and the dimensions actually assessed.

Study	Context and biological units	Measurements and principal findings	Evidence coverage and interpretation
Marschallinger et al. 2020 Physiological aging [15, 124, 125]	Male C57BL/6J mice, mainly 2–4 versus 18–20 months. Dentate-gyrus BODIPY assay: n = 6 mice/group; CARS: n = 5/group; reported lipidomics: n = 4 mice/group. Aging RNA-seq used n = 3 samples/group, each pooling three mice. Human hippocampal images illustrated 22- and 67-year-old individuals; sex/cohort size was not specified in the legend.	BODIPY/TMEM119, PLIN3, EM, CARS, sorted-cell transcriptomics, droplet lipidomics, ROS, and uptake assays. BODIPY-positive microglia: 12.08% versus 51.95%; CARS: 18.93% versus 50.76%. Article text reports 44.4% glycerolipids and 0.7% CE in aged-microglial droplets.	Structure and transcription measured; oxidative/metabolic and uptake abnormalities measured. Static lipidomics is not turnover. Zymosan acidification and labeled-myelin uptake do not alone establish completed degradation. Quantitative screen interpretation follows the correction notice.
Marschallinger et al. 2020 Genetic/inflammatory comparisons [15, 124]	Male Grn-null mice at 9–10 months with WT littermates; hippocampus. Histology n = 5 mice/group; zymosan uptake n = 3/group. Grn-null RNA-seq used n = 3 independent samples/group, each pooling two mice. BV2 screen and LPS experiments were separate systems; approximately 2,000 genes screened, 112 regulators using the corrected criterion.	Grn-null hippocampal microglia had about twice the proportion of droplet-positive cells and twice the droplets/cell. Selected gene deletions altered droplet burden, ROS, and zymosan uptake. LPS also induced droplets in young mice.	Supports lysosomal/trafficking and inflammatory routes to the phenotype. Gene deletion, chronological aging, and stimulated immortalized cells are not interchangeable conditions.
Shimabukuro et al. 2016 Aging lipid-laden cells [126]	Female BALB/c mice: 3, 12, and 18–22 months. Regional density comparisons: n = 3 mice/group. Cortex, striatum, pia, and ventricular/neurogenic regions.	Oil Red O and perilipin with IBA1, NeuN, GFAP, or S100β; LC3/beclin-1, TNF, and β-galactosidase. Lipid-laden cells increased with age and included several cellular identities.	Structural and marker-based evidence. Autophagy markers do not establish lipophagic flux. The multi-cell population should not be relabeled wholesale as microglial LDAM.

Gouna et al. 2021 Demyelination and repair [102]	Male WT, Trem2-null, and Soat1-null mice, 9–15 weeks; focal spinal demyelination. Principal lesion experiments: n = 3–4 animals/condition, with time point specified per assay.	PLIN2, lipid/cholesterol measurements, lysosomal/ER-stress readouts, and myelin-repair endpoints. TREM2/SOAT1 deficiency impaired adaptive droplet formation and resolution of the lesion response.	Direct perturbation and tissue-repair evidence for an adaptive storage response. Young-adult demyelination is a mechanistic comparator, not physiological-aging LDAM.
Arbaizar-Rovirosa et al. 2023 Aging and ischemia [127]	C57BL/6 mice: 3–4 versus 21–22 months. Brain-hemisphere microglia, with striatal lesion imaging. Female RNA-seq: young n = 7, old n = 5. Flow cytometry: sham n = 3 and ischemia n = 4 per age/sex group; male and female groups distinguished.	CD11b/CD45/BODIPY sorting, PLIN2, EM, RNA-seq, and pHrodo bacterial-particle uptake; ischemia assessed at 4 days. Microglial renewal reduced age-associated lipid/inflammatory features.	Structural, transcriptional, and functional comparisons. Renewal can replace cells, so improvement does not prove recovery of the original lipid-loaded cells. Ischemia introduces a defined injury context.
Haney et al. 2024 Human tissue [21]	Frontal cortex. Supplementary Table 1 lists control APOE3/3: n = 8, age 80–101, M/F 4/4; AD APOE3/3: n = 8, age 70–101, M/F 3/5; AD APOE4/4: n = 10, age 64–84, M/F 6/4. These metadata counts are distinct from individual histology panels.	snRNA-seq identified an ACSL1-associated state. ACSL1/IBA1 histology used n = 5 subjects/group. Oil Red O comparisons used control n = 12, AD33 n = 7, AD44 n = 9. Histological neutral-lipid identity was not resolved for every stained cell.	Human structural/transcriptional association. No direct in vivo turnover or task-recovery measurement. Cohort age distributions and separate assay subsets must be retained; cells/nuclei are not independent donors.
Haney et al. 2024 Cell models [21]	APOE-genotyped human induced microglia plus separate BV2 and U937 assays. BV2 13C-to-TAG incorporation: n = 3 wells/condition; induced-microglial zymosan uptake: n = 4 wells/condition. Well replication is not donor replication.	Aβ-associated lipids, ACSL1, labeled TAG synthesis, RNA/ATAC-seq, CRISPR screens, uptake, conditioned-medium neurotoxicity, and GNE-317 response.	Cell-model mechanisms and cellular effects. Synthesis was measured in a specified cell system; it should not be reported as human postmortem flux. GNE-317-associated LC3B changes did not prove lipophagic completion.
Prakash et al. 2025 Aβ–DGAT2 [23]	Ex vivo: 5–7-month female WT/5xFAD microglia; n = 4 experiments for Fig. 5b and n = 3 for c/e/f. In vivo subiculum: 11–24 months; n = 8 degrader and n = 5 vehicle for plaque/droplet analyses. Neuritic-dystrophy panel: male, n = 8 versus 4. Sex distribution is not explicit for every in vivo panel.	Neutral-lipid dyes, Raman imaging, lipidomics/metabolomics, Dgat2 perturbation, Aβ-pHrodo, and pathology. Ex vivo droplets decreased 51–57%; uptake increased 1.41-fold in droplet-positive 5xFAD cells. In vivo pathology changed after local infusion.	Composition, perturbation, uptake, and tissue-pathology evidence. Mass changes are not flux, and pHrodo is not a completed-degradation chase. Inhibitor exposure and intracerebroventricular degrader delivery are separate arms.
Huynh et al. 2024 Myelin-loaded cells [22]	Human HMC3 and murine N9 lines; 24-h myelin loading. HMC3 Figure 3: myelin at 25 µg/mL cholesterol equivalent, N = 3–6 as reported. Biological age/sex cannot be inferred from the immortalized line; the legend does not further resolve each replicate type.	3H-oleate incorporation into CE/TAG, TLC lipid mass, Nile Red, PLIN2, ABCA1, and LXR antagonism. CE synthesis and free cholesterol were distinguished from total neutral-lipid staining.	Direct synthesis and lipid-mass data. ABCA1 induction is not a measured net-efflux rate. Cell-line identity and substrate loading limit extrapolation to aged resident microglia.
Huynh et al. 2024 APOE-targeted-replacement aging [48]	Female mice, 9 and 16–20 months; forebrain homogenates. Animal group n is not explicitly specified in the corresponding figure legends. The cellular arm reported 40 cells/group for imaging and n = 3 for Western blots.	Systemic nanoparticle F12511 for 13–14 days; bulk TLR4, cytokines, PLIN2, and ABCA1. Neonatal primary-microglial experiments were distinct from the aged in vivo experiment.	Age-defined inflammatory pharmacodynamics. A bulk-tissue marker trend does not establish microglial droplet or flux rescue; image-cell counts must not be treated as independent animals.

Han et al. 2025 TBK1–ACSL1 [77]	BV2 drug assay: n = 3 independent experiments in Fig. 6. Male C57BL/6 mice, 6–8 weeks, in LPS/MPTP arms; substantia nigra and striatum. In vivo histology n = 5 mice/group; ER-ACSL1 and immunoblots n = 3/group. Public human substantia-nigra datasets supplied a separate disease association.	GSK8612, siRNA, kinase-inactive TBK1, interaction/ubiquitination and localization assays; droplet and inflammatory outcomes. In vivo treatment improved selected nigrostriatal and motor readouts with reduced microglial ER-ACSL1. Drug conditions are given in Table 3.	Signaling, pharmacodynamic and selected tissue/functional evidence. Drug concentration in brain was not measured; systemic dosing plus central pharmacodynamics does not specify exposure or cell-exclusive action. No physiological-aging or completed-clearance comparison.
Claes et al. 2021 Human microglia in chimeric AD mice [104]	7-month 5X-hCSF1 hosts with WT or TREM2-R47H human microglia. scRNA-seq: WT n = 3 and R47H n = 2 mice. PLIN2 histology used female hosts, n = 4 WT and n = 3 R47H, with 5–6 images/mouse; dorsal subiculum and CA1. Plaque-proximity analyses also sampled retrosplenial granular cortex.	Human-cell transcription, plaque proximity, PLIN2, CD9, and APOE. R47H cells showed reduced total plaque-associated PLIN2 and reduced plaque engagement; the proportion of plaque-near cells forming droplets was not different.	Structural/transcriptional and spatial-response evidence. Reduced staining can reflect altered recruitment/engagement, without demonstrating improved intracellular disposal.
Victor et al. 2022 APOE4 and neuronal surveillance [105]	Human induced-microglial isogenic models derived from a 75-year-old female APOE3/3 donor and a separate 70-year-old female AD APOE4/4 donor. RNA-seq used n = 3 biological replicates. Donor age is not the biological age of the reprogrammed cells.	Lipid accumulation, transcriptional/metabolic profiles, and responses to neuronal-network activity were linked in microglia–neuron experiments. Isogenic editing and a second donor background tested APOE-associated effects.	Cell-resolved lipid and functional evidence. Reprogramming, culture maturation, and donor background constrain extrapolation to naturally aged human microglia. Assay-specific replication is retained rather than equating wells to donors.
TCW et al. 2022 APOE4 glial cholesterol handling [72]	Population and isogenic human iPSC-derived glia; the isogenic series included four sex-balanced donors and 24 clones, three clones/genotype/donor. Cellular maturation and donor identity, not a mouse-equivalent chronological age, define these models.	Cell-type transcriptomics, lysosomal cholesterol localization, lipid metabolism, and perturbation experiments showed substantial donor and APOE-haplotype variation. Microglia, astrocytes, and neuronal cultures were analyzed separately.	Mechanistic and donor-resolved evidence for glial lipid dysregulation. A shared APOE genotype did not eliminate background effects, and lysosomal cholesterol staining alone is not completed cholesterol export.

Note. Animal/donor replication is distinguished from cells, fields and wells. Human donor inventory and panel-specific histological subsets remain separate. The table records available observations without a validated LDAM score. ALS tissue lipidomics and motor-neuron ferroptosis remain disease comparators in Section 6.5 [78–80], rather than direct microglial LDAM studies.
Direct tracer-incorporation measurements of synthesis are distinguished from static lipid mass, staining and expression markers. Missing experimental metadata are retained as not specified rather than imputed.
Note. Sample sizes are assay-specific biological units. A marker or transcriptomic result is distinguished from a direct turnover or functional measurement. Structural, transcriptional, metabolic, and functional coverage describes available evidence rather than a validated diagnostic score. An unmeasured dimension remains unknown. Direct tracer-incorporation measurements of synthesis are distinguished from static lipid mass, staining and expression markers. Missing experimental metadata are retained as not specified rather than imputed.
Abbreviations: Aβ, amyloid-β; ACSL1, acyl-CoA synthetase long-chain family member 1; AD, Alzheimer's disease; ALS, amyotrophic lateral sclerosis; APOE, apolipoprotein E; CE, cholesteryl ester; DGAT2, diacylglycerol acyltransferase 2; ER, endoplasmic reticulum; iPSC, induced pluripotent stem cell; LDAM, lipid-droplet-accumulating microglia; MRI, magnetic resonance imaging; PD, Parkinson's disease; ROS, reactive oxygen species; TAG, triacylglycerol; TBK1, TANK-binding kinase 1; TREM2, triggering receptor expressed on myeloid cells 2.

7. Biological insights from spatial and multi-omics studies

Spatial and multi-omics studies can identify where substrate supply and processing demand are concentrated. Their value for the present model is to locate candidate populations and connect anatomical context to lipid species and functional measurements. Figure 3 and Supplementary Table S1 organize complementary assays around this biological question.

7.1 Single-cell states and population composition

Single-cell and single-nucleus transcriptomics reveal microglial heterogeneity in aging and disease [97, 98, 135]. Analyses need to separate shifts in state abundance from expression changes within a state and account for isolation bias. Pairing transcriptomics with imaging or post-sorting droplet and functional measurements connects response programs to lipid phenotypes.

7.2 Empirical spatial biology of aging white matter

White-matter studies identify anatomically restricted phagocytic and inflammatory responses during aging [99-101]. Wang and colleagues compared young, middle-aged, and old mice of both sexes and identified white-matter fiber tracts as a prominent site of microglial, astroglial, complement, and myeloid-infiltration signatures [136]. Immunofluorescence and quantitative MRI associated these changes with myelin loss and sex-dependent effects. The spatial results locate a high-demand niche; droplet imaging, lipid-species measurements, and processing assays are then needed to establish its lipid phenotype. AD lesion neighborhoods offer a separate anatomical comparison [137, 138].

7.3 Lipidomics complements flux measurements

Regional lipidomics identifies heterogeneous brain composition and aging-related remodeling [8, 24, 139]. Cell-resolved measurement of CE, TAG, free fatty acids, membrane phospholipids, and oxidized species can connect that environment to microglial storage. Isotope incorporation and disappearance during a chase period then distinguish synthesis from mobilization and disposal. Together, these measurements can test whether a white-matter niche predominantly increases cholesterol input, restricts export, or alters fatty-acid processing.

7.4 Localization limits of spatial lipidomics

MALDI or DESI mass-spectrometry imaging localizes lipid signals, with cell assignment constrained by spatial resolution, ionization efficiency, and molecular annotation [140, 141]. Registration with cell markers, myelin, and droplet imaging, followed by targeted molecular confirmation, can characterize the local substrates within inflammatory white-matter regions.

7.5 Communication inference versus measured lipid transfer

CellChat and related methods infer candidate communication from ligand–receptor expression [142] and can prioritize APOE-, complement-, or survival-related interactions [143]. These predictions identify where receptor perturbation or labeled-lipid transfer experiments may be informative. Measurements of receptor signaling, including SYK activity, are needed to connect predicted communication to a processing reaction in the responding microglia.

Regional human lipidomics [139], the ssREAD AD resource [144], and brain-wide mouse-aging transcriptomics [145] supply complementary atlas data. Linking these resources requires retaining age, sex, region, genotype, pathology, and the measurements available for each population. A study-resolved atlas could then reveal comparable populations and prioritize the reactions that still require experimental testing.

Figure 3 organizes these complementary sources and measurements around the biological questions they can address.

8. Pharmacological intervention: Mechanisms and strength of evidence

Intervention assessment begins with the substrate, reaction, and cellular task evaluated in the original experiment. Table 3 records tested interventions, doses, durations, target-validation evidence, and outcomes. Figure 4 relates those observations to the additional requirements for translation to brain aging.

8.1 Evidence strength and evaluation endpoints

Evidence is assessed along two separate axes: causal support for the target in the studied model, and applicability to physiological-aging LDAM. A genetic or pharmacological perturbation can strongly support a disease-model mechanism without establishing that the same target limits processing during aging. Aging-related pathway changes provide direct age context but may lack cell-resolved metabolic or functional endpoints. Stimulated-cell and peripheral-macrophage findings generate more indirect leads. A human therapy that combines microglial target engagement, multidimensional LDAM assessment, and functional recovery is not established in the literature considered here.

Target engagement, functional improvement, and therapeutic efficacy are distinct claims. Droplet abundance, substrate incorporation, uptake, completed degradation, and neuronal or tissue benefit should be reported separately. A pharmacodynamic response or benefit in a cell-culture or disease model does not establish therapeutic efficacy in physiological brain aging. Comparisons must retain dose, duration, route, brain exposure, and cell-resolved target evidence.

APOE genotype, TREM2–SYK signaling competence, local substrates, and residual organelle function help identify the context in which a target may be limiting.

8.2 Target-supported interventions in lipid handling

In myelin-loaded HMC3 and N9 cells, K604 or F12511 at 0.5 μM for 24 h inhibited CE synthesis; the HMC3 experiments measured lower free cholesterol and CE together with increased ABCA1 expression [22].

GSK2033 blocked ABCA1 induction, supporting an LXR-dependent transcriptional response. F12511 also reduced droplets and increased ABCA1 protein in neonatal APOE4 primary microglia, whereas its in vivo aging experiment used 46 mg/kg nanoparticle-formulated F12511 daily for 13–14 days in female APOE-targeted-replacement mice, including a 16–20-month-old group [48]. TLR4 and selected cytokines decreased in forebrain homogenates; PLIN2 showed a trend and bulk ABCA1 was unchanged. The experiment did not establish microglial lipid turnover or cognitive recovery. F12511 inhibits ACAT/SOAT enzymes and is not strictly SOAT1-selective; isoform specificity and delivery evidence are therefore recorded separately from its measured inflammatory effects.

DGAT2 was tested through complementary perturbations: genetic reduction, the inhibitor D2i (Sigma PZ0233), and an in-house protein degrader [23]. Ex vivo assays used 15 μM D2i with a 1-h pretreatment before a 30-min amyloid-uptake assay. The in vivo experiment infused 120 μM degrader into the lateral ventricle at 1 μL/h for seven days. Reduced microglial DGAT2 protein supports target engagement after local delivery, but this route does not establish systemic blood–brain barrier penetration. TREM2-directed strategies raise a different issue: apolipoprotein binding and amyloid uptake are supported by ligand studies [146], while cholesterol retention after chronic challenge was established in a separate TREM2-deficiency study [14]. These functions should not be inferred from receptor abundance alone.

8.3 Targeting organelle processing capacity

TFEB-regulated lysosomal programs and autophagy studies motivate investigation of organelle-directed interventions [56, 58, 120]. In APOE4/4 induced microglia, a CRISPR screen identified PIK3CA, and 10 μM GNE-317 for 24 h during fibrillar Aβ exposure reduced lipid-droplet and lysosomal accumulation and altered inflammatory output [21]. Increased LC3B and expression of autophagy-related genes accompanied this response. As acknowledged in the original study, these static measurements do not demonstrate increased autophagic flux. The cellular target result therefore supports a PI3K-associated response in this model while leaving completed lipophagy and systemic brain exposure unresolved.

The TBK1 study also tested GSK8612 in vivo [77]. The LPS-model timeline used 10 mg/kg/day for seven days; the MPTP arm specified intraperitoneal 10 mg/kg/day from day 0 to day 14. Treatment reduced inflammatory readouts and TH-positive cell loss in the nigrostriatal system. Reduced ER-associated ACSL1 in sorted substantia-nigra microglia and lower tissue p-TBK1 supported a pharmacodynamic response; tissue PLIN3 also decreased in the LPS arm. Histological comparisons used n = 5 mice/group and the ER-ACSL1 and immunoblot comparisons n = 3/group. Selected motor outcomes improved, but the MPTP dopamine comparison and LPS pole-test comparison did not reach significance. These results extend beyond the BV2 experiments without supplying quantitative brain drug concentrations or a direct test of completed lipid disposal. Table 3 distinguishes the cellular and in vivo regimens. Total TBK1 reduction and kinase inhibition had different localization effects, so the corresponding perturbations should be interpreted separately.

8.4 Inflammatory and redox interventions in disease models

MCC950 improved amyloid-related clearance and cognitive outcomes in APP/PS1 mice [147], supporting a role for NLRP3 in that disease setting. Inflammasome and autophagy reviews place these findings within broader inflammatory mechanisms [118, 120]. Their interpretation remains tied to the measured inflammatory and functional endpoints; an effect on the reaction responsible for lipid retention requires additional metabolic evidence.

8.5 Indirect pharmacological leads from natural products

Selected natural-product studies report inflammatory or autophagy-associated effects in LPS and disease models [148-151], while a recent trilobatin study directly assessed microglial lipid dysregulation after traumatic brain injury [152]. These context-specific leads do not establish recovery of physiological-aging LDAM and should be evaluated with the same exposure, target, lipid-processing, and functional criteria as other interventions.

8.6 Toward translation

Translation begins by relating effective concentrations to measured brain exposure and identifying the responding cells and target. It then requires recovery of the implicated lipid-processing reaction and cellular task, followed by evaluation of tissue or cognitive benefit. Age, sex, genotype, and region need prospective consideration. For chemically complex preparations, active constituents, purity, batch composition, and metabolites must also be characterized.

Safety includes preservation of membrane-lipid homeostasis and necessary phagocytic functions. Improved cellular processing must be connected to tissue or cognitive benefit before an intervention can be

considered relevant to brain aging. Figure 4 presents this validation sequence as a research workflow.

9. Outstanding questions

The main unresolved questions concern which reaction fails in a defined aging population, how that population arises, and whether its original cells can recover. Addressing these questions requires joint metabolic and functional measurements over time.

The original aging-LDAM study supplies a quantitative reference phenotype [15]. Replication should retain the animal or donor as the biological unit, report droplet distributions and assay conditions, and distinguish changes in state abundance from changes within individual cells. Agreement across structural and functional measurements can then be tested across centers before diagnostic thresholds are proposed.

Longitudinal experiments can connect state origin to recovery. Retained population labels and repeated metabolic or functional measurements would show whether the original lipid-loaded cells improve, die, or are replaced after substrate withdrawal or treatment.

White-matter fiber tracts offer a focused anatomical setting. Repeated measurements of myelin injury, resident and infiltrating cells, lipid composition, and disposal can test whether increasing substrate supply precedes the processing defect. Cell-specific perturbation of esterification or export would identify the limiting reaction rather than inferring it from regional inflammation.

Human aging studies need age, sex, APOE genotype, region, comorbidities, postmortem interval, and neuropathological burden. Matched histology and single-nucleus profiles can establish spatial and transcriptional associations; perturbable human-derived models can test candidate reactions. The resulting observations should retain the distinction between naturally aged tissue and a reprogrammed cell model.

Computational analyses can prioritize these experiments, provided the original context and assumptions remain visible. Independent measurements of transfer, signaling, turnover, or lineage must test the specific relationship being inferred.

Three comparisons make the organizing model testable. First, matched droplet burdens can be compared for lipid composition and completed clearance. Second, inhibition of esterification can be assessed for the joint fate of stored and free substrates and the recovery of the impaired task. Third, increased uptake can be evaluated together with downstream degradation and export. These comparisons identify the conditions under which a proposed intervention improves processing, shifts the retained substrate, or fails. A disagreement between predicted and observed outcomes should revise the mechanistic interpretation.

10. Conclusion

Microglial lipid droplets in brain aging have to be interpreted with their composition, substrate source, and measured cellular function. Primary studies support both adaptive storage during myelin repair and dysfunctional lipid retention in selected aging and disease settings. Their intervention results differ in target, delivery route, and endpoint. Study-resolved comparisons and the proposed reporting checklist keep those differences and unmeasured dimensions explicit. Future work can use them to identify the limiting reaction, test safe disposal, and connect microglial recovery to neural benefit. The reporting framework and conditional predictions remain open to validation.

Author Contributions

Xintong Wang: Conceptualization, literature search and synthesis, visualization, and writing of the original draft. Yu Tian: Literature search, literature screening, and revision. Dongna Li: Literature review, critical analysis and synthesis, and revision. Xueji Fan, Yuqian Wang, Anran Lv: Literature search, reference organization, and revision. Pengwei Zhuang: Conceptualization, supervision, manuscript coordination, and writing of the original draft. Yanjun Zhang: Supervision, critical review, and review and editing. All authors are accountable for their respective contributions.

Declaration of competing interest

The authors declare that they have no known competing financial interests or personal relationships that could have influenced this work.

Funding

This work was supported by the Tianjin Outstanding Talent Program (Grant No. JC20230415) and the Tianjin Education Commission for Higher Education (Grant No. 2024KJ035).

Declaration of AI-assisted illustration and language editing

The authors used ChatGPT (OpenAI) to generate schematic illustration elements and to assist with language editing. The figure elements were assembled and edited by the authors in Microsoft PowerPoint. The figures are conceptual schematics and do not represent experimental data. The authors reviewed and edited the

AI-assisted content and take responsibility for its accuracy and final presentation.

References

[1] López-Otín C, Blasco MA, Partridge L, Serrano M, Kroemer G (2023). Hallmarks of aging: An expanding universe. Cell, 186:243-278.

[2] Partridge L, Deelen J, Slagboom PE (2018). Facing up to the global challenges of ageing. Nature, 561:45-56.

[3] Mattson MP, Arumugam TV (2018). Hallmarks of Brain Aging: Adaptive and Pathological Modification by Metabolic States. Cell Metab, 27:1176-1199.

[4] Wyss-Coray T (2016). Ageing, neurodegeneration and brain rejuvenation. Nature, 539:180-186.

[5] Colonna M, Butovsky O (2017). Microglia Function in the Central Nervous System During Health and Neurodegeneration. Annu Rev Immunol, 35:441-468.

[6] Deczkowska A, Keren-Shaul H, Weiner A, Colonna M, Schwartz M, Amit I (2018). Disease-Associated Microglia: A Universal Immune Sensor of Neurodegeneration. Cell, 173:1073-1081.

[7] Raulin AC, Martens YA, Bu G (2022). Lipoproteins in the Central Nervous System: From Biology to Pathobiology. Annu Rev Biochem, 91:731-759.

[8] Yoon JH, Seo Y, Jo YS, Lee S, Cho E, Cazenave-Gassiot A, et al. (2022). Brain lipidomics: From functional landscape to clinical significance. Sci Adv, 8:eadc9317.

[9] Cantuti-Castelvetri L, Fitzner D, Bosch-Queralt M, Weil MT, Su M, Sen P, et al. (2018). Defective cholesterol clearance limits remyelination in the aged central nervous system. Science, 359:684-688.

[10] Sun Y, Wei K, Liao X, Wang J, Gao L, Pang B (2025). Lipid metabolism in microglia: Emerging mechanisms and therapeutic opportunities for neurodegenerative diseases (Review). Int J Mol Med, 56:139.

[11] Tiwari V, Simons M (2025). Lipid metabolism and neuroinflammation: What is the link? J Exp Med, 222:e20241232.

[12] Wu S, Liu X, Yang H, Ma W, Qin Z (2023). The effect of lipid metabolism on age-associated cognitive decline: Lessons learned from model organisms and human. IBRO Neurosci Rep, 15:165-169.

[13] Krasemann S, Madore C, Cialic R, Baufeld C, Calcagno N, El Fatimy R, et al. (2017). The TREM2-APOE Pathway Drives the Transcriptional Phenotype of Dysfunctional Microglia in Neurodegenerative Diseases. Immunity, 47:566-581.e9.

[14] Nugent AA, Lin K, van Lengerich B, Lianoglou S, Przybyla L, Davis SS, et al. (2020). TREM2 Regulates Microglial Cholesterol Metabolism upon Chronic Phagocytic Challenge. Neuron, 105:837-854.e9.

[15] Marschallinger J, Iram T, Zardeneta M, Lee SE, Lehallier B, Haney MS, et al. (2020). Lipid-droplet-accumulating microglia represent a dysfunctional and proinflammatory state in the aging brain. Nat Neurosci, 23:194-208.

[16] Sung S, Kim HJ, Cha SJ, Nahm M, Kim SH, Kwon MS (2026). Microglial lipid droplets as therapeutic targets in age-related neurodegenerative diseases. NPJ Aging, 12:2.

[17] Prakash P, Randolph CE, Walker KA, Chopra G (2025). Lipids: Emerging Players of Microglial Biology. Glia, 73:657-677.

[18] Fu L, Luo T, Hao Z, Pan Y, Xin W, Zhang L, et al. (2025). Exploring novel roles of lipid droplets and lipid metabolism in regulating inflammation and blood-brain barrier function in neurological diseases. Front Neurosci, 19:1603292.

[19] Guo S, Zhang Q, Guo R, Fu L, Zhu H, Zhang Q (2026). Lipid Droplet-Accumulating Microglia as a Therapeutic Node in Neurodegenerative Disease. ACS Chem Neurosci, 17:2302-2318.

[20] Rana M, Ko WC, Nepali K, Ko CY, Yen TL, Jan JS, et al. (2026). Glial lipid reprogramming in brain aging: Lipid identity, organelle stress, and redox vulnerability. Redox Biol, 98:104453.

[21] Haney MS, Pálovics R, Munson CN, Long C, Johansson PK, Yip O, et al. (2024). APOE4/4 is linked to damaging lipid droplets in Alzheimer's disease microglia. Nature, 628:154-161.

[22] Huynh TN, Havrda MC, Zanazzi GJ, Chang CCY, Chang TY (2024). Inhibiting the Cholesterol Storage Enzyme ACAT1/SOAT1 in Myelin Debris-Treated Microglial Cell Lines Activates the Gene Expression of Cholesterol Efflux Transporter ABCA1. Biomolecules, 14:1301.

[23] Prakash P, Manchanda P, Paouri E, Bisht K, Sharma K, Rajpoot J, et al. (2025). Amyloid-β induces lipid droplet-mediated microglial dysfunction via the enzyme DGAT2 in Alzheimer's disease. Immunity, 58:1536-1552.e8.

[24] Cerasuolo M, Di Meo I, Auriemma MC, Paolisso G, Papa M, Rizzo MR (2024). Exploring the Dynamic Changes of Brain Lipids, Lipid Rafts, and Lipid Droplets in Aging and Alzheimer's Disease. Biomolecules, 14:1362.

[25] Björkhem I, Meaney S (2004). Brain cholesterol: long secret life behind a barrier. Arterioscler Thromb Vasc Biol, 24:806-815.

[26] Dietschy JM, Turley SD (2004). Thematic review series: brain Lipids. Cholesterol metabolism in the central nervous system during early development and in the mature animal. J Lipid Res, 45:1375-1397.

[27] Pfrieger FW (2003). Cholesterol homeostasis and function in neurons of the central nervous system. Cell Mol Life Sci, 60:1158-1171.

[28] Nunes VS, da Silva Ferreira G, Quintão ECR (2022). Cholesterol metabolism in aging simultaneously altered in liver and nervous system. Aging (Albany NY), 14:1549-1561.

[29] Saher G (2023). Cholesterol Metabolism in Aging and Age-Related Disorders. Annu Rev Neurosci, 46:59-78.

[30] Hannun YA, Obeid LM (2008). Principles of bioactive lipid signalling: lessons from sphingolipids. Nat Rev Mol Cell Biol, 9:139-150.

[31] van Meer G, Voelker DR, Feigenson GW (2008). Membrane lipids: where they are and how they behave. Nat Rev Mol Cell Biol, 9:112-124.
[32] Dadsena S, Hassan DG, Holthuis JCM (2019). Unraveling the molecular principles by which ceramides commit cells to death. Cell Stress, 3:280-283.
[33] Farooqui AA, Horrocks LA, Farooqui T (2000). Glycerophospholipids in brain: their metabolism, incorporation into membranes, functions, and involvement in neurological disorders. Chem Phys Lipids, 106:1-29.
[34] Harayama T, Riezman H (2018). Understanding the diversity of membrane lipid composition. Nat Rev Mol Cell Biol, 19:281-296.
[35] van Meer G, de Kroon AI (2011). Lipid map of the mammalian cell. J Cell Sci, 124:5-8.
[36] Emre C, Do KV, Jun B, Hjorth E, Alcalde SG, Kautzmann MI, et al. (2021). Age-related changes in brain phospholipids and bioactive lipids in the APP knock-in mouse model of Alzheimer's disease. Acta Neuropathol Commun, 9:116.
[37] Narzt MS, Kremslehner C, Golabi B, Nagelreiter IM, Malikovic J, Hussein AM, et al. (2022). Molecular species of oxidized phospholipids in brain differentiate between learning- and memory impaired and unimpaired aged rats. Amino Acids, 54:1311-1326.
[38] Bazinet RP, Layé S (2014). Polyunsaturated fatty acids and their metabolites in brain function and disease. Nat Rev Neurosci, 15:771-785.
[39] Dyall SC (2015). Long-chain omega-3 fatty acids and the brain: a review of the independent and shared effects of EPA, DPA and DHA. Front Aging Neurosci, 7:52.
[40] Lauritzen L, Brambilla P, Mazzocchi A, Harsløf LB, Ciappolino V, Agostoni C (2016). DHA Effects in Brain Development and Function. Nutrients, 8:6.
[41] Cutuli D (2017). Functional and Structural Benefits Induced by Omega-3 Polyunsaturated Fatty Acids During Aging. Curr Neuropharmacol, 15:534-542.
[42] Denis I, Potier B, Vancassel S, Heberden C, Lavialle M (2013). Omega-3 fatty acids and brain resistance to ageing and stress: body of evidence and possible mechanisms. Ageing Res Rev, 12:579-594.
[43] Shichiri M (2014). The role of lipid peroxidation in neurological disorders. J Clin Biochem Nutr, 54:151-160.
[44] Brown MS, Goldstein JL (1997). The SREBP pathway: regulation of cholesterol metabolism by proteolysis of a membrane-bound transcription factor. Cell, 89:331-340.
[45] Chitraju C, Walther TC, Farese RV Jr (2019). The triglyceride synthesis enzymes DGAT1 and DGAT2 have distinct and overlapping functions in adipocytes. J Lipid Res, 60:1112-1120.
[46] Horton JD, Goldstein JL, Brown MS (2002). SREBPs: activators of the complete program of cholesterol and fatty acid synthesis in the liver. J Clin Invest, 109:1125-1131.
[47] Olzmann JA, Carvalho P (2019). Dynamics and functions of lipid droplets. Nat Rev Mol Cell Biol, 20:137-155.
[48] Huynh TN, Fikse EN, De La Torre AL, Havrda MC, Chang CCY, Chang TY (2024). Inhibiting the Cholesterol Storage Enzyme ACAT1/SOAT1 in Aging Apolipoprotein E4 Mice Alters Their Brains' Inflammatory Profiles. Int J Mol Sci, 25:13690.
[49] Kim WS, Rahmanto AS, Kamili A, Rye KA, Guillemin GJ, Gelissen IC, et al. (2007). Role of ABCG1 and ABCA1 in regulation of neuronal cholesterol efflux to apolipoprotein E discs and suppression of amyloid-beta peptide generation. J Biol Chem, 282:2851-2861.
[50] Koldamova R, Fitz NF, Lefterov I (2014). ATP-binding cassette transporter A1: from metabolism to neurodegeneration. Neurobiol Dis, 72 Pt A:13-21.
[51] Wuerch EC, Yong VW (2025). Cholesterol in the CNS: functions, recycling and remyelination. J Neuroinflammation, 22:180.
[52] Sardiello M, Palmieri M, di Ronza A, Medina DL, Valenza M, Gennarino VA, et al. (2009). A gene network regulating lysosomal biogenesis and function. Science, 325:473-477.
[53] Settembre C, Di Malta C, Polito VA, Garcia Arencibia M, Vetrini F, Erdin S, et al. (2011). TFEB links autophagy to lysosomal biogenesis. Science, 332:1429-1433.
[54] Singh R, Kaushik S, Wang Y, Xiang Y, Novak I, Komatsu M, et al. (2009). Autophagy regulates lipid metabolism. Nature, 458:1131-1135.
[55] Carmona-Gutierrez D, Hughes AL, Madeo F, Ruckenstuhl C (2016). The crucial impact of lysosomes in aging and longevity. Ageing Res Rev, 32:2-12.
[56] Nixon RA (2020). The aging lysosome: An essential catalyst for late-onset neurodegenerative diseases. Biochim Biophys Acta Proteins Proteom, 1868:140443.
[57] Li Q, Zhao Y, Guo H, Li Q, Yan C, Li Y, et al. (2023). Impaired lipophagy induced-microglial lipid droplets accumulation contributes to the buildup of TREM1 in diabetes-associated cognitive impairment. Autophagy, 19:2639-2656.
[58] Xu Y, Propson NE, Du S, Xiong W, Zheng H (2021). Autophagy deficiency modulates microglial lipid homeostasis and aggravates tau pathology and spreading. Proc Natl Acad Sci U S A, 118:e2023418118.
[59] Bartman S, Coppotelli G, Ross JM (2024). Mitochondrial Dysfunction: A Key Player in Brain Aging and Diseases. Curr Issues Mol Biol, 46:1987-2026.
[60] Li Y, Zhao T, Li J, Xia M, Li Y, Wang X, et al. (2022). Oxidative Stress and 4-hydroxy-2-nonenal (4-HNE): Implications in the Pathogenesis and Treatment of Aging-related Diseases. J Immunol Res, 2022:2233906.
[61] Dixon SJ, Lemberg KM, Lamprecht MR, Skouta R, Zaitsev EM, Gleason CE, et al. (2012). Ferroptosis: an iron-dependent form of nonapoptotic cell death. Cell, 149:1060-1072.
[62] Fei Y, Ding Y (2024). The role of ferroptosis in neurodegenerative diseases. Front Cell Neurosci, 18:1475934.
[63] Stockwell BR, Friedmann Angeli JP, Bayir H, Bush AI, Conrad M, Dixon SJ, et al. (2017). Ferroptosis: A

Regulated Cell Death Nexus Linking Metabolism, Redox Biology, and Disease. Cell, 171:273-285.

[64] Couttas TA, Kain N, Tran C, Chatterton Z, Kwok JB, Don AS (2018). Age-Dependent Changes to Sphingolipid Balance in the Human Hippocampus are Gender-Specific and May Sensitize to Neurodegeneration. J Alzheimers Dis, 63:503-514.

[65] Pamplona R, Borras C, Jové M, Pradas I, Ferrer I, Viña J (2019). Redox lipidomics to better understand brain aging and function. Free Radic Biol Med, 144:310-321.

[66] Ralhan I, Chang CL, Lippincott-Schwartz J, Ioannou MS (2021). Lipid droplets in the nervous system. J Cell Biol, 220:e202102136.

[67] Tan D, Konduri S, Erikci Ertunc M, Zhang P, Wang J, Chang T, et al. (2023). A class of anti-inflammatory lipids decrease with aging in the central nervous system. Nat Chem Biol, 19:187-197.

[68] Tu J, Yin Y, Xu M, Wang R, Zhu ZJ (2017). Absolute quantitative lipidomics reveals lipidome-wide alterations in aging brain. Metabolomics, 14:5.

[69] Shin KC, Ali Moussa HY, Park Y (2024). Cholesterol imbalance and neurotransmission defects in neurodegeneration. Exp Mol Med, 56:1685-1690.

[70] Zhang X, Chen C, Liu Y (2024). Navigating the metabolic maze: anomalies in fatty acid and cholesterol processes in Alzheimer's astrocytes. Alzheimers Res Ther, 16:63.

[71] Ioannou MS, Jackson J, Sheu SH, Chang CL, Weigel AV, Liu H, et al. (2019). Neuron-Astrocyte Metabolic Coupling Protects against Activity-Induced Fatty Acid Toxicity. Cell, 177:1522-1535.e14.

[72] Tcw J, Qian L, Pipalia NH, Chao MJ, Liang SA, Shi Y, et al. (2022). Cholesterol and matrisome pathways dysregulated in astrocytes and microglia. Cell, 185:2213-2233.e25.

[73] Di Paolo G, Kim TW (2011). Linking lipids to Alzheimer's disease: cholesterol and beyond. Nat Rev Neurosci, 12:284-296.

[74] Keren-Shaul H, Spinrad A, Weiner A, Matcovitch-Natan O, Dvir-Szternfeld R, Ulland TK, et al. (2017). A Unique Microglia Type Associated with Restricting Development of Alzheimer's Disease. Cell, 169:1276-1290.e17.

[75] Andersen C, Grønnemose AL, Pedersen JN, Nowak JS, Christiansen G, Nielsen J, et al. (2021). Lipid Peroxidation Products HNE and ONE Promote and Stabilize Alpha-Synuclein Oligomers by Chemical Modifications. Biochemistry, 60:3644-3658.

[76] Galvagnion C (2017). The Role of Lipids Interacting with α-Synuclein in the Pathogenesis of Parkinson's Disease. J Parkinsons Dis, 7:433-450.

[77] Han C, Wang H, Zhang M, Wu L, Wang A, Yang P, et al. (2025). Activated TBK1 promotes ACSL1-mediated microglia lipid droplet accumulation and neuroinflammation in Parkinson's disease. J Neuroinflammation, 22:190.

[78] Chaves-Filho AB, Pinto IFD, Dantas LS, Xavier AM, Inague A, Faria RL, et al. (2019). Alterations in lipid metabolism of spinal cord linked to amyotrophic lateral sclerosis. Sci Rep, 9:11642.

[79] Goutman SA, Guo K, Savelieff MG, Patterson A, Sakowski SA, Habra H, et al. (2022). Metabolomics identifies shared lipid pathways in independent amyotrophic lateral sclerosis cohorts. Brain, 145:4425-4439.

[80] Wang T, Tomas D, Perera ND, Cuic B, Luikinga S, Viden A, et al. (2022). Ferroptosis mediates selective motor neuron death in amyotrophic lateral sclerosis. Cell Death Differ, 29:1187-1198.

[81] Antignano I, Liu Y, Offermann N, Capasso M (2023). Aging microglia. Cell Mol Life Sci, 80:126.

[82] Gao C, Jiang J, Tan Y, Chen S (2023). Microglia in neurodegenerative diseases: mechanism and potential therapeutic targets. Signal Transduct Target Ther, 8:359.

[83] Loving BA, Bruce KD (2020). Lipid and Lipoprotein Metabolism in Microglia. Front Physiol, 11:393.

[84] Bedolla A, Wegman E, Weed M, Stevens MK, Ware K, Paranjpe A, et al. (2024). Adult microglial TGFβ1 is required for microglia homeostasis via an autocrine mechanism to maintain cognitive function in mice. Nat Commun, 15:5306.

[85] Butovsky O, Weiner HL (2018). Microglial signatures and their role in health and disease. Nat Rev Neurosci, 19:622-635.

[86] Butovsky O, Jedrychowski MP, Moore CS, Cialic R, Lanser AJ, Gabriely G, et al. (2014). Identification of a unique TGF-β-dependent molecular and functional signature in microglia. Nat Neurosci, 17:131-143.

[87] Ishikawa K, Fujikawa R, Okita K, Kimura F, Watanabe T, Katsurabayashi S, et al. (2025). Microglia in Brain Aging and Age-Related Diseases: Friends or Foes? Int J Mol Sci, 26:11494.

[88] Cao G, Bales KR, DeMattos RB, Paul SM (2007). Liver X receptor-mediated gene regulation and cholesterol homeostasis in brain: relevance to Alzheimer's disease therapeutics. Curr Alzheimer Res, 4:179-184.

[89] Wang Y, Cella M, Mallinson K, Ulrich JD, Young KL, Robinette ML, et al. (2015). TREM2 lipid sensing sustains the microglial response in an Alzheimer's disease model. Cell, 160:1061-1071.

[90] Boisvert MM, Erikson GA, Shokhirev MN, Allen NJ (2018). The Aging Astrocyte Transcriptome from Multiple Regions of the Mouse Brain. Cell Rep, 22:269-285.

[91] Guttenplan KA, Weigel MK, Prakash P, Wijewardhane PR, Hasel P, Rufen-Blanchette U, et al. (2021). Neurotoxic reactive astrocytes induce cell death via saturated lipids. Nature, 599:102-107.

[92] Liddelow SA, Guttenplan KA, Clarke LE, Bennett FC, Bohlen CJ, Schirmer L, et al. (2017). Neurotoxic reactive astrocytes are induced by activated microglia. Nature, 541:481-487.

[93] Jung ES, Choi H, Mook-Jung I (2025). Decoding microglial immunometabolism: a new frontier in Alzheimer's disease research. Mol Neurodegener, 20:37.

[94] Lauro C, Limatola C (2020). Metabolic Reprograming of Microglia in the Regulation of the Innate Inflammatory Response. Front Immunol, 11:493.

[95] Miao J, Chen L, Pan X, Li L, Zhao B, Lan J (2023). Microglial Metabolic Reprogramming: Emerging Insights and Therapeutic Strategies in Neurodegenerative Diseases. Cell Mol Neurobiol, 43:3191-3210.

[96] Nakamura Y, Nakano M, Hisaoka-Nakashima K, Morioka N (2025). Aging-related dysregulation of energy metabolism and mitochondrial dynamics in microglia. J Clin Biochem Nutr, 76:239-244.

[97] Hammond TR, Dufort C, Dissing-Olesen L, Giera S, Young A, Wysoker A, et al. (2019). Single-Cell RNA Sequencing of Microglia throughout the Mouse Lifespan and in the Injured Brain Reveals Complex Cell-State Changes. Immunity, 50:253-271.e6.

[98] Masuda T, Sankowski R, Staszewski O, Böttcher C, Amann L, Sagar, et al. (2019). Spatial and temporal heterogeneity of mouse and human microglia at single-cell resolution. Nature, 566:388-392.

[99] Safaiyan S, Besson-Girard S, Kaya T, Cantuti-Castelvetri L, Liu L, Ji H, et al. (2021). White matter aging drives microglial diversity. Neuron, 109:1100-1117.e10.

[100] Kaya T, Mattugini N, Liu L, Ji H, Cantuti-Castelvetri L, Wu J, et al. (2022). CD8(+) T cells induce interferon-responsive oligodendrocytes and microglia in white matter aging. Nat Neurosci, 25:1446-1457.

[101] Safaiyan S, Kannaiyan N, Snaidero N, Brioschi S, Biber K, Yona S, et al. (2016). Age-related myelin degradation burdens the clearance function of microglia during aging. Nat Neurosci, 19:995-998.

[102] Gouna G, Klose C, Bosch-Queralt M, Liu L, Gokce O, Schifferer M, et al. (2021). TREM2-dependent lipid droplet biogenesis in phagocytes is required for remyelination. J Exp Med, 218:e20210227.

[103] Li RY, Qin Q, Yang HC, Wang YY, Mi YX, Yin YS, et al. (2022). TREM2 in the pathogenesis of AD: a lipid metabolism regulator and potential metabolic therapeutic target. Mol Neurodegener, 17:40.

[104] Claes C, Danhash EP, Hasselmann J, Chadarevian JP, Shabestari SK, England WE, et al. (2021). Plaque-associated human microglia accumulate lipid droplets in a chimeric model of Alzheimer's disease. Mol Neurodegener, 16:50.

[105] Victor MB, Leary N, Luna X, Meharena HS, Scannail AN, Bozzelli PL, et al. (2022). Lipid accumulation induced by APOE4 impairs microglial surveillance of neuronal-network activity. Cell Stem Cell, 29:1197-1212.e8.

[106] Wang S, Sudan R, Peng V, Zhou Y, Du S, Yuede CM, et al. (2022). TREM2 drives microglia response to amyloid-β via SYK-dependent and -independent pathways. Cell, 185:4153-4169.e19.

[107] Melo RC, Weller PF (2016). Lipid droplets in leukocytes: Organelles linked to inflammatory responses. Exp Cell Res, 340:193-197.

[108] Fourgeaud L, Través PG, Tufail Y, Leal-Bailey H, Lew ED, Burrola PG, et al. (2016). TAM receptors regulate multiple features of microglial physiology. Nature, 532:240-244.

[109] Nguyen LT, Aprico A, Nwoke E, Walsh AD, Blades F, Avneri R, et al. (2023). Mertk-expressing microglia influence oligodendrogenesis and myelin modelling in the CNS. J Neuroinflammation, 20:253.

[110] Duewell P, Kono H, Rayner KJ, Sirois CM, Vladimer G, Bauernfeind FG, et al. (2010). NLRP3 inflammasomes are required for atherogenesis and activated by cholesterol crystals. Nature, 464:1357-1361.

[111] Rajamäki K, Lappalainen J, Oörni K, Välimäki E, Matikainen S, Kovanen PT, et al. (2010). Cholesterol crystals activate the NLRP3 inflammasome in human macrophages: a novel link between cholesterol metabolism and inflammation. PLoS One, 5:e11765.

[112] Yvan-Charvet L, Wang N, Tall AR (2010). Role of HDL, ABCA1, and ABCG1 transporters in cholesterol efflux and immune responses. Arterioscler Thromb Vasc Biol, 30:139-143.

[113] Byrns CN, Perlegos AE, Miller KN, Jin Z, Carranza FR, Manchandra P, et al. (2024). Senescent glia link mitochondrial dysfunction and lipid accumulation. Nature, 630:475-483.

[114] Byrns CN, Perlegos AE, Miller KN, Jin Z, Carranza FR, Manchandra P, et al. (2024). Author Correction: Senescent glia link mitochondrial dysfunction and lipid accumulation. Nature, 632:E8.

[115] Ng PY, McNeely TL, Baker DJ (2023). Untangling senescent and damage-associated microglia in the aging and diseased brain. FEBS J, 290:1326-1339.

[116] Rim C, You MJ, Nahm M, Kwon MS (2024). Emerging role of senescent microglia in brain aging-related neurodegenerative diseases. Transl Neurodegener, 13:10.

[117] Franceschi C, Garagnani P, Parini P, Giuliani C, Santoro A (2018). Inflammaging: a new immune-metabolic viewpoint for age-related diseases. Nat Rev Endocrinol, 14:576-590.

[118] Heneka MT, McManus RM, Latz E (2018). Inflammasome signalling in brain function and neurodegenerative disease. Nat Rev Neurosci, 19:610-621.

[119] Zheng Y, Sun J, Luo Z, Li Y, Huang Y (2024). Emerging mechanisms of lipid peroxidation in regulated cell death and its physiological implications. Cell Death Dis, 15:859.

[120] Lin M, Yu H, Xie Q, Xu Z, Shang P (2022). Role of microglia autophagy and mitophagy in age-related neurodegenerative diseases. Front Aging Neurosci, 14:1100133.

[121] Zhou X, Wang J, Yu L, Qiao G, Qin D, Yuen-Kwan Law B, et al. (2024). Mitophagy and cGAS-STING crosstalk in neuroinflammation. Acta Pharm Sin B, 14:3327-3361.

[122] Klionsky DJ, Abdel-Aziz AK, Abdelfatah S, Abdellatif M, Abdoli A, Abel S, et al. (2021). Guidelines for the use and interpretation of assays for monitoring autophagy (4th edition). Autophagy, 17:1-382.

[123] Hambright WS, Fonseca RS, Chen L, Na R, Ran Q (2017). Ablation of ferroptosis regulator glutathione peroxidase 4 in forebrain neurons promotes cognitive impairment and neurodegeneration. Redox Biol, 12:8-17.

[124] Marschallinger J, Iram T, Zardeneta M, Lee SE, Lehallier B, Haney MS, et al. (2020). Author Correction: Lipid-droplet-accumulating microglia represent a dysfunctional and proinflammatory state in the aging brain. Nat Neurosci, 23:294.

[125] Marschallinger J, Iram T, Zardeneta M, Lee SE, Lehallier B, Haney MS, et al. (2020). Author Correction: Lipid-droplet-accumulating microglia represent a dysfunctional and proinflammatory state in the aging brain. Nat Neurosci, 23:1308.

[126] Shimabukuro MK, Langhi LG, Cordeiro I, Brito JM, Batista CM, Mattson MP, et al. (2016). Lipid-laden cells differentially distributed in the aging brain are functionally active and correspond to distinct phenotypes. Sci Rep, 6:23795.

[127] Arbaizar-Rovirosa M, Pedragosa J, Lozano JJ, Casal C, Pol A, Gallizioli M, et al. (2023). Aged lipid-laden microglia display impaired responses to stroke. EMBO Mol Med, 15:e17175.

[128] Vicidomini C, Goode TD, Yu R, Mehta I, McAvoy KM, Beveridge CH, et al. (2026). An aging-sensitive secreted phospholipase confers neuroprotection and cognitive resilience. Nat Neurosci. Advance online publication. https://doi.org/10.1038/s41593-026-02465-z.

[129] Logan T, Simon MJ, Rana A, Cherf GM, Srivastava A, Davis SS, et al. (2021). Rescue of a lysosomal storage disorder caused by Grn loss of function with a brain penetrant progranulin biologic. Cell, 184:4651-4668.e25.

[130] Logan T, Simon MJ, Rana A, Cherf GM, Srivastava A, Davis SS, et al. (2024). Rescue of a lysosomal storage disorder caused by Grn loss of function with a brain penetrant progranulin biologic. Cell, 187:1565-1566.

[131] Stephens IO, Johnson LA (2025). Knockout of Perilipin-2 in Microglia Alters Lipid Droplet Accumulation and Response to Alzheimer's Disease Stimuli. Cells, 14:1783.

[132] Maiyo BK, Loppi SH, Morrison HW, Doyle KP (2024). Assessment and Quantification of Foam Cells and Lipid Droplet-Accumulating Microglia in Mouse Brain Tissue Using BODIPY Staining. Bio Protoc, 14:e5107.

[133] Mazzulli JR, Xu YH, Sun Y, Knight AL, McLean PJ, Caldwell GA, et al. (2011). Gaucher disease glucocerebrosidase and α-synuclein form a bidirectional pathogenic loop in synucleinopathies. Cell, 146:37-52.

[134] Bonet-Ponce L, Beilina A, Williamson CD, Lindberg E, Kluss JH, Saez-Atienzar S, et al. (2020). LRRK2 mediates tubulation and vesicle sorting from lysosomes. Sci Adv, 6:eabb2454.

[135] Stanley N, Dhawka L, Jaikumar S, Huang YC, Zannas AS (2025). Microglia Single-Cell RNA-Seq Enables Robust and Applicable Markers of Biological Aging. Aging Cell, 24:e70095.

[136] Wang L, Cui CY, Lee CT, Bodogai M, Yang N, Shi C, et al. (2025). Spatial transcriptomics of the aging mouse brain reveals origins of inflammation in the white matter. Nat Commun, 16:3231.

[137] Miyoshi E, Morabito S, Henningfield CM, Das S, Rahimzadeh N, Shabestari SK, et al. (2024). Spatial and single-nucleus transcriptomic analysis of genetic and sporadic forms of Alzheimer's disease. Nat Genet, 56:2704-2717.

[138] Zhou Y, Glass CK (2025). Microglia networks within the tapestry of alzheimer's disease through spatial transcriptomics. Mol Neurodegener, 20:102.

[139] Osetrova M, Tkachev A, Mair W, Guijarro Larraz P, Efimova O, Kurochkin I, et al. (2024). Lipidome atlas of the adult human brain. Nat Commun, 15:4455.

[140] Jha D, Blennow K, Zetterberg H, Savas JN, Hanrieder J (2024). Spatial neurolipidomics-MALDI mass spectrometry imaging of lipids in brain pathologies. J Mass Spectrom, 59:e5008.

[141] Leontyev D, Pulliam AN, Ma X, Gaul DA, LaPlaca MC, Fernández FM (2024). Spatial lipidomics maps brain alterations associated with mild traumatic brain injury. Front Chem, 12:1394064.

[142] Jin S, Guerrero-Juarez CF, Zhang L, Chang I, Ramos R, Kuan CH, et al. (2021). Inference and analysis of cell-cell communication using CellChat. Nat Commun, 12:1088.

[143] Wu Y, Eisel ULM (2023). Microglia-Astrocyte Communication in Alzheimer's Disease. J Alzheimers Dis, 95:785-803.

[144] Wang C, Acosta D, McNutt M, Bian J, Ma A, Fu H, et al. (2024). A single-cell and spatial RNA-seq database for Alzheimer's disease (ssREAD). Nat Commun, 15:4710.

[145] Jin K, Yao Z, van Velthoven CTJ, Kaplan ES, Glattfelder K, Barlow ST, et al. (2025). Brain-wide cell-type-specific transcriptomic signatures of healthy ageing in mice. Nature, 638:182-196.

[146] Yeh FL, Wang Y, Tom I, Gonzalez LC, Sheng M (2016). TREM2 Binds to Apolipoproteins, Including APOE and CLU/APOJ, and Thereby Facilitates Uptake of Amyloid-Beta by Microglia. Neuron, 91:328-340.

[147] Dempsey C, Rubio Araiz A, Bryson KJ, Finucane O, Larkin C, Mills EL, et al. (2017). Inhibiting the NLRP3 inflammasome with MCC950 promotes non-phlogistic clearance of amyloid-β and cognitive function in APP/PS1 mice. Brain Behav Immun, 61:306-316.

[148] Han X, Xu T, Fang Q, Zhang H, Yue L, Hu G, et al. (2021). Quercetin hinders microglial activation to alleviate neurotoxicity via the interplay between NLRP3 inflammasome and mitophagy. Redox Biol, 44:102010.

[149] Huang S, Liu H, Lin Y, Liu M, Li Y, Mao H, et al. (2020). Berberine Protects Against NLRP3 Inflammasome via Ameliorating Autophagic Impairment in MPTP-Induced Parkinson's Disease Model. Front Pharmacol, 11:618787.

[150] Jiang P, Guo Y, Dang R, Yang M, Liao D, Li H, et al. (2017). Salvianolic acid B protects against lipopolysaccharide-induced behavioral deficits and neuroinflammatory response: involvement of autophagy

and NLRP3 inflammasome. J Neuroinflammation, 14:239.

[151] Jin X, Liu MY, Zhang DF, Zhong X, Du K, Qian P, et al. (2019). Baicalin mitigates cognitive impairment and protects neurons from microglia-mediated neuroinflammation via suppressing NLRP3 inflammasomes and TLR4/NF-κB signaling pathway. CNS Neurosci Ther, 25:575-590.

[152] Zhang HW, Wang XJ, Chu MM, Xing GY, Qiu K, Zhang YG, et al. (2026). SLC27A3-dependent lipid metabolic reprogramming by trilobatin suppresses microglial mtDNA/TLR9-driven inflammatory activation in traumatic brain injury. J Neuroinflammation, 23:255.